INTERNATIONAL JOURNAL FOR NUMERICAL METHODS IN ENGINEERING
Int. J. Numer. Meth. Engng 2000; **00**:1–6 *Prepared using* nmeauth.cls *[Version: 2002/09/18 v2.02]*

The extended/generalized finite element method: An overview of the method and its applications

Thomas-Peter Fries*[1†] and Ted Belytschko[2‡]

[1] *Thomas-Peter Fries, Chair for Computational Analysis of Technical Systems, RWTH Aachen University, Schinkelstr. 2, 52062 Aachen, Germany*
[2] *Department of Mechanical Engineering, Northwestern University, 2145 Sheridan Road, Evanston, IL 60208, U.S.A.*

SUMMARY

An overview of the extended/generalized finite element method with emphasis on methodological issues is presented. This method enables the accurate approximation of solutions that involve jumps, kinks, singularities, and other locally non-smooth features within elements. This is achieved by enriching the polynomial approximation space of the classical finite element method. The extended/generalized finite element method has shown its potential in a variety of applications that involve non-smooth solutions near interfaces: Among them are the simulation of cracks, shear bands, dislocations, solidification, and multi-field problems. Copyright © 2000 John Wiley & Sons, Ltd.

KEY WORDS: Review, Extended Finite Element Method, XFEM, Generalized Finite Element Method, GFEM, Partition of Unity Method, PUM

1. Introduction

A large number of examples can be found in the real world where field quantities change rapidly over length scales that are small with respect to the observed domain. For the modeling of such phenomena, the resulting solutions typically involve discontinuities, singularities, high gradients or other non-smooth properties. In solid mechanics, we find examples for non-smooth solutions in models for cracks, shear bands, dislocations, inclusions, and voids. In fluid mechanics, locally non-smooth solutions are found in shocks, boundary layers and near interfaces in multi-phase flows.

For the approximation of non-smooth solutions, there are two fundamentally different approaches: The first strategy uses *polynomial* approximation spaces and relies on meshes that

*Correspondence to: Thomas-Peter Fries, Chair for Computational Analysis of Technical Systems, RWTH Aachen University, Schinkelstr. 2, 52062 Aachen, Germany
†E-mail: fries@cats.rwth-aachen.de
‡E-mail: tedbelytschko@northwestern.edu

Contract/grant sponsor: German Research Foundation; contract/grant number: 0

Received 23 October 2009

conform to discontinuities and are refined near singularities and high gradients. To treat the evolution of such phenomena, remeshing is required. An efficient way to construct polynomial approximation spaces is given by classical finite element (FE) shape functions [28, 203]. We note also that many meshfree shape functions rely on the approximation properties of polynomials [27, 80], so there is a great flexibility in the construction of polynomial approximation spaces.

The second strategy is to *enrich* a polynomial approximation space such that the non-smooth solutions can be modeled *independent of the mesh*. Methods that extend polynomial approximation spaces are called "enriched methods" in this work. The enrichment can be achieved by adding special shape functions (which are customized so as to capture jumps, singularities, etc.) to the polynomial approximation space. This is called "extrinsic enrichment" and more shape functions and unknowns result in the approximation. An alternative for the enrichment is to replace (at least some of) the shape functions in the polynomial approximation space by special shape functions that can capture non-smooth solutions. This approach is called "intrinsic enrichment" and the number of shape functions and unknowns is unchanged. For enriched methods, we further distinguish between enrichments in the whole domain or in local subregions only. Global enrichments are for example useful for high-frequency solutions of the Helmholtz equation, i.e. when the solution can be considered globally non-smooth. However, most non-smooth solution properties such as jumps, kinks, and singularities are local phenomena and it is then natural to employ the enrichment in local subdomains.

One may thus extract (at least) three criteria for the classification of enriched methods: (i) The shape functions (including those of the enrichments) are meshfree or meshbased, (ii) the enrichment extrinsic or intrinsic, and (iii) the enrichment is realized globally or locally.

Intrinsic, local enrichments may be found in a meshfree context e.g. by Fleming *et al.* [75]. In a meshbased context, this kind of enrichments has been proposed by Fries and Belytschko [78] for the "intrinsic XFEM" (local enrichment) and [79] for the "intrinsic PUM" (global enrichment). In the rest of this work, intrinsic enrichments of approximations will not be discussed.

We here focus on *meshbased* enrichment methods which realize the enrichment *extrinsically* by the partition of unity concept. These methods include the partition of unity method (PUM) [16, 117, 92] the generalized finite element method (GFEM) [169, 171], and the extended finite element method (XFEM) [23, 126]. Previous surveys on the XFEM are by Karihaloo and Xiao [104], Abdelaziz and Hamouine [2], Belytschko *et al.* [26], and Rabczuk *et al.* [146]. A monograph on the XFEM has been published by Mohammadi [128]. This book and the aforementioned surveys deal primarily with applications of the XFEM in solid mechanics, mostly in fracture. A survey of the generalized finite element method dealing with the mathematical aspects is included in Babuška *et al.* [13] along with meshfree methods.

This overview concentrates on *methodological* issues that arise in XFEM; many of these topics also apply to PUM and GFEM. These issues include boundary and interface constraints, numerical integration, blending elements, error estimation, time-integration, higher-order extensions, etc. Previous surveys have often been structured with respect to applications and mention these methodological issues separately in different places. In contrast, this survey is structured systematically with respect to the methodological issues. In addition, we also survey the multitude of applications to which the XFEM has been successfully applied so far. In the description of these applications, however, the emphasis is on the method rather than on the governing equations and the modeling.

1.1. PUM, GFEM, and XFEM

The PUM, GFEM, and XFEM are closely related in that the extrinsic enrichments used in these methods have the same structure. The enrichment is realized through the partition of unity (PU) concept, which was proposed by Babuška *et al.* [14]. The fantastic possibilities of this approach were first elaborated by Babuška and Melenk in [16, 117]. They called their method the partition of unity method (PUM) or the partition of unity finite element method (PUFEM). These works dealt with global enrichments such as harmonic polynomials for the Laplace and Helmholtz equations, and holomorphic functions for linear elasticity. Also, general enrichments of low order partition of unities with higher-order polynomials were realized. These "polynomial enrichments" through partition of unities are also central to the *hp*-cloud method by Duarte and Oden [66, 64, 136]. In these works, the aim of the enrichments was the improvement of the general approximation properties in the entire domain as compared to classical FE approximations. The enrichment for capturing locally non-smooth phenomena was envisioned though not further elaborated (with the exception of enrichments for boundary layers as discussed in [16]). All of the approaches mentioned so far are applicable to meshfree and meshbased PUs. Meshbased PUs are for example defined by Lagrange finite elements, meshfree PUs are constructed by Shepard functions [160] or moving least-squares functions [110, 27, 80].

In the aforementioned works, the generality of the methods is stressed. However, the construction of the PUs and the numerical integration of the weak form can be drastically different. Meshfree PUs in the frame of the moving-least squares method are well-known to be computationally expensive and are notoriously difficult to integrate, whereas, meshbased PUs are easily constructed by Lagrange elements and quadrature of the weak form is simple. For efficiency, it is desirable to retain as much as possible from the classical FEM in the PUM. This is the motivation for the generalized finite element method by Strouboulis and Babuška [169] ("a combination of the classical FEM and the PUM") and of the XFEM of Moës *et al.* [126]. The PU in these methods is furnished by standard FE shape functions. The GFEM was first applied in [169, 171, 172, 174, 170, 173] to different elliptic problems (most often the Laplace equation) with voids; these works also provide a mathematical background of the GFEM. The enrichment functions used are sometimes numerically computed functions ("handbook" functions) that include characteristic local behavior. Analytical enrichments are used in a similar manner as in the PUM, in particular methods with polynomial and harmonic polynomial enrichments are reported.

It is noted that the name GFEM has already been cited in [17, 15] in a very general way with no specific relation to PUs: "This method covers practically all modifications of the FEM which lead to a sparse system matrix.". However, herein the name GFEM is used in the sense of Strouboulis *et al.* [169].

XFEM also employs PUs provided by conventional FE functions, see Belytschko and Black [23] and Moës *et al.* [126]. A feature which distinguishes the XFEM from the early work in GFEM is that only local parts of the domain are enriched and this localization is achieved by enriching a *subset of the nodes*. Furthermore, enrichments which capture arbitrary discontinuities and non-smooth functions were developed in the XFEM framework in Moës *et al.* [126] which dealt with linear elastic fracture mechanics. Later, the XFEM was also used for general interface phenomena e.g. in the framework of multi-material problems [178], solidification [50], shear bands [7], dislocations [25], and multi-field problems [207]. The

important features that characterize XFEM are: (i) The enrichment is *extrinsic* and realized by the PU concept, (ii) the enrichment is *local* because only a subset of the nodes is enriched, (iii) the enrichment is *meshbased*, i.e. the PU is constructed by means of standard FE shape functions, and (iv) enrichments for arbitrary discontinuities in the function and their gradients are available.

These attributes are also present in some later realizations of the GFEM and PUM, see for example [196, 162]. *In this work, wherever we use the term XFEM, the same applies for the GFEM and PUM as long as they use meshbased shape functions and local enrichments.* The name GFEM has been used for methods that range from the PUM (e.g. [63] where meshfree Shepard functions as well as FE functions are employed) to XFEM-like methods (e.g. [162] which is not distinguishable from the XFEM). Thus the distinctions between PUM, GFEM, and XFEM have become quite fuzzy; in a sense, as the names are used today, they are almost identical methods.

1.2. Related methods

Other meshbased methods that are used for the approximation of fields with discontinuities and/or high gradients are briefly mentioned here: In the discontinuous enrichment method (DEM) of Farhat *et al.* [39], the standard FEM space is enriched within each element by additional non-conforming functions. The degrees of freedom that are associated with the enrichment are statically condensed on the element level, that is, no additional unknowns result through the enrichment. However, Lagrange multipliers are introduced in order to enforce continuity between elements. It is interesting to note that: (i) in the XFEM/GFEM/PUM, unknowns of the standard FEM and the enrichment are present in the final system of equations, (ii) in the DEM, standard FEM unknowns and Lagrange multipliers exist, (iii) in the intrinsic XFEM [78], only standard FEM unknowns are present. On the other hand, the number of unknowns is clearly not the only measure for efficiency. One has to also take into account the effort for the static condensation and the construction of the Lagrange multiplier space in the DEM, or the effort for computing the enriched moving-least squares functions in the intrinsic XFEM. For more information on the DEM, the interested reader is refered to works by Farhat and coworkers [72, 41, 40, 99, 140, 145, 107].

The concept of mesh independent approximations for non-smooth solutions also involves the weak element method, see Rose [153] and Goldstein [86], the ultra weak variational method of Cessenat and Depres [42], the least-squares method as proposed in [129], the global-local FEM as described by Mote [130] and Noor [134]. Finally, we mention the manifold method as proposed by Shi [161], see also Chen *et al.* [44], which can model arbitrary closed discontinuities; but for open discontinuities that end within the domain, the method requires continuity constraints, which can be imposed by Lagrange multipliers.

1.3. Structure of the paper

In section 2, we give examples where discontinuities and high gradients are observed in reality and models. These features are often found locally across interfaces. The description of interfaces in domains is discussed in section 3. The level-set method is typically used in the XFEM for the description as it also simplifies the construction of the enrichment. The structure of approximations as frequently used in the PUM, GFEM, and XFEM is described in section 4. It is seen that the definition of enrichment functions and a corresponding set of

enriched nodes characterize a particular application of the XFEM. Typical choices depending on different phenomena (jumps, kinks, high gradients, etc.) are given in section 5 together with an overview of related applications.

When using enriched approximations, a number of additional issues arise which are discussed in the subsequent sections: Section 6 focuses on the quadrature of the weak form, section 7 on higher-order results, section 8 on time-integration issues in the XFEM, section 9 on the enforcement of boundary and interface conditions, section 10 on error estimation and adaptivity, section 11 on linear dependencies and ill-conditioning, and section 12 on the implementation of the XFEM. The paper ends in section 13 with conclusions.

2. Discontinuities and high gradients

In the real world, there are numerous examples where field quantities and/or their gradients change rapidly over length scales Δl that are small compared to the dimensions of the observed domain. We consider three characteristic cases which are important for the *modeling* of the phenomena: (i) Δl is zero as for the example of cracks, (ii) Δl is extremely small so that it is justified to idealize it as a discontinuity in models, and (iii) Δl is small but has to be considered in models leading to locally high gradients. For the rest of the work, we associate the term "discontinuity" with the cases (i) and (ii) and the term "high gradient" with case (iii). High gradients also occur in the vicinity of singularities and other problems.

2.1. Interfaces

Consider a d-dimensional domain $\Omega \in \mathbb{R}^d$. An "interface" is a manifold $\Gamma \in \mathbb{R}^{d-1}$ inside the domain. That is, in a two-dimensional domain, interfaces are lines; in a three-dimensional domain, interfaces are surfaces. One may classify *open* and *closed* interfaces depending on whether they end inside the domain or not, see Fig. 1. Furthermore, we distinguish between *moving* and *fixed* interfaces. Fixed interfaces are, for example, material interfaces in a solid when treated by Lagrangian descriptions. Although the solid deforms, the relative position of the interface does not change. The situation differs for the example of material interfaces in two-phase flows in terms of Eulerian coordinates. Then, the interface is moving with respect to the coordinates and a successive update of the interface is needed during the simulation. Additional models are required for the consideration of moving interfaces.

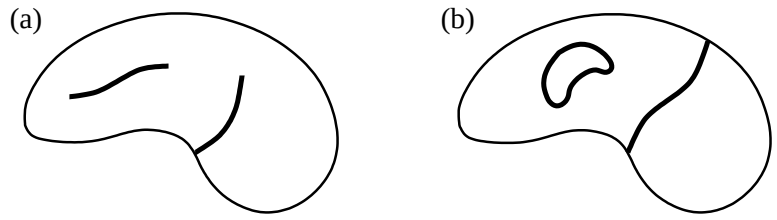

Figure 1. Example for (a) open and (b) closed interfaces.

2.2. Discontinuities

Solutions of models with *strong* discontinuities have jumps across interfaces. The variables on both sides of the interface are decoupled, so that their gradients are also discontinuous across the interface. An example may be seen in Fig. 2(a). Solutions with *weak* discontinuities have kinks across interfaces, i.e. only the gradients are discontinuous, whereas the solution is continuous, see Fig. 2(b).

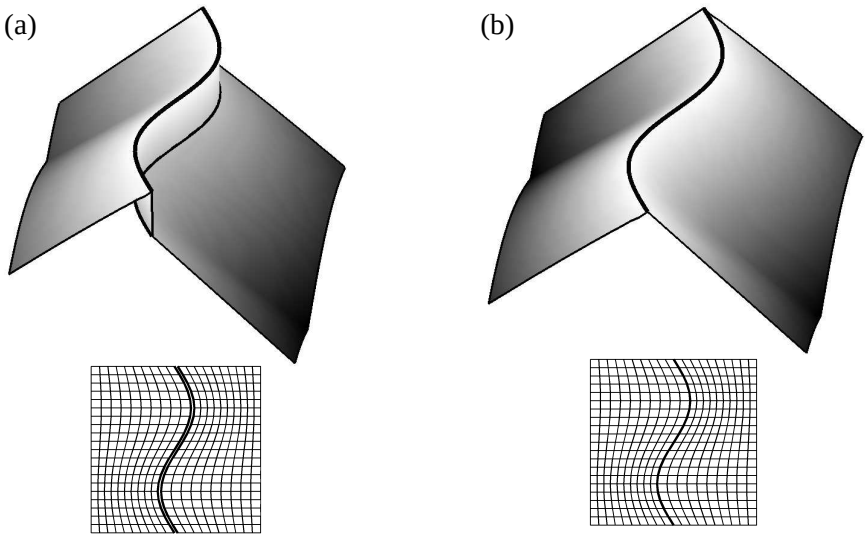

Figure 2. Example for a (a) strong and (b) weak discontinuity across an interface. Below are suitable meshes for a classical FE simulation.

Let us briefly mention how discontinuities are treated within the classical FEM. The classical FEM relies on the approximation properties of (mapped) polynomials. Optimal accuracy is achieved for *smooth* solutions. Thus, inner-element jumps and kinks lead to a drastic decrease of accuracy. It is, therefore, crucial in the classical FEM to align the element edges of the mesh with the interfaces where strong and weak discontinuities appear. Furthermore, for strong discontinuities, a complete decoupling of the elements next to the interface is important. In applications where the interfaces are moving, the mesh has to be updated so that the elements always align with the interface (interface tracking). See Fig. 2 for examples of meshes that can be used for a classical FE simulation of discontinuities.

2.3. High gradients

High gradients may appear either in the vicinity of points or lines, e.g. in case of singularities, or across interfaces. In the latter case, the interface is usually placed so its position coincides with the maximum gradient. This interface can either be inside the domain or coincide with parts of the boundary. See Fig. 3(a)-(c) for examples.

High gradients in the classical FEM require an appropriate refinement of the mesh; see for example in Fig. 3. This refinement can lead to a large increase in the computational effort. Furthermore, mesh refinement is often not a fully automatic procedure and user-controlled

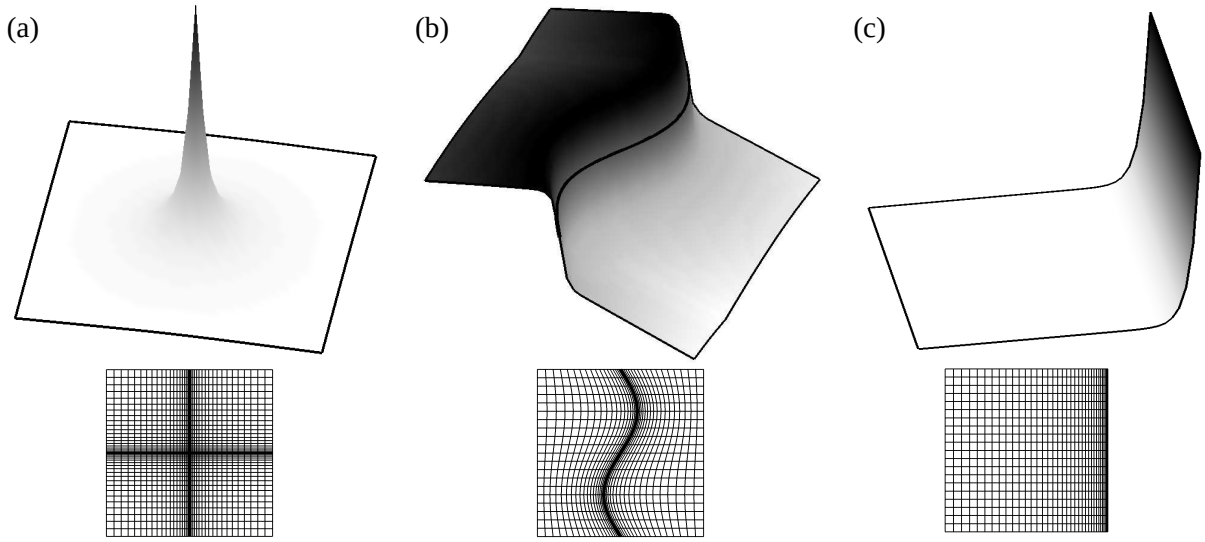

Figure 3. Example for high gradients: (a) a singularity, (b) a high gradient across an interface, (c) a high gradient near the boundary. Below are suitable meshes for a classical FE simulation.

adjustments are required.

2.4. Examples

We give some examples where discontinuities and high gradients are frequently encountered in models. Material interfaces and phase boundaries are examples where discontinuities are present across closed interfaces. The solutions of crack problems are discontinuous across open interfaces. At the crack tip, the stresses and strains are often singular. In the problem of propagating cracks, the interfaces evolve with time.

Shear bands and dislocations have displacement fields which are discontinuous in the tangential direction of an open interface. Sometimes it is appropriate to consider the shear band width, then, rather a high gradient is encountered. Shocks and boundary layers are examples which are particularly important in fluid mechanics, where high gradients are present inside the domain or at the boundary.

2.5. Motivation for XFEM

We conclude that local, non-smooth solutions with discontinuities and high gradients occur frequently in physical problems. The classical FEM relies on the construction of meshes that align with the discontinuities and are refined near high gradients. In the modeling of evolution problems, the classical FEM requires remeshing. An alternative is to *enrich the approximation space* of the FEM such that these non-smooth solution properties are accounted for correctly, independent of the mesh. This is the path chosen in the XFEM. As a consequence, simple, fixed meshes can be used throughout the simulation and mesh construction and maintenance are reduced to a minimum.

3. Description of interfaces

In order to enrich the approximation space in the XFEM appropriately, an accurate description of the interface positions in the domain is useful. The level-set method [138, 137, 159] has proven to be an ideal complement to the XFEM. By means of the level-set method, it is not only possible to determine *where* the enrichment is needed but it also facilitates the construction of the enrichment, as shall be seen later. This method defines interfaces implicitly by means of the zero-level of a scalar function within the domain. XFEM was first combined with level sets in Belytschko *et al.* [29] and Stolarska *et al.* [167].

Remark: Explicit interface descriptions.

It is noted that the level-set method is not a necessary part of the XFEM. For example, in [23, 126] cracks in two-dimensional domains have been parametrized explicitly by polygons. The same is done for arbitrary branched and intersecting cracks in Daux *et al.* [55]. In Duarte *et al.* [63] and Sukumar *et al.* [180], crack surfaces in three-dimensional domains are described by a set of connected planes. However, determining the intersection of the parametrized lines/surfaces with the mesh is not an easy task, see [180] for computational details. Interfaces can also be described by Bézier splines and NURBS, which enable *smooth* interface representations.

3.1. Closed interfaces

Let us assume the domain $\Omega \in \mathbb{R}^d$ falls into two different regions Ω_1 and Ω_2 such that $\Omega = \Omega_1 \cup \Omega_2$ and $\Omega_1 \cap \Omega_2 = \Gamma_{12}$. The normal vector on the interface Γ_{12} is denoted by $\boldsymbol{n}$, see Fig. 4(a). A level-set function is any continuous function $\phi(\boldsymbol{x})$, $\boldsymbol{x} \in \Omega$, that is negative in one subdomain and positive in the other. The zero-level of this function is the position of the closed interface Γ_{12}, i.e.

$$\Gamma_{12} = \{\boldsymbol{x} : \ \phi(\boldsymbol{x}) = 0\}. \tag{1}$$

The *signed distance function* [138] is a particularly useful level-set function,

$$\phi(\boldsymbol{x}) = \pm \min_{\boldsymbol{x}^\star \in \Gamma_{12}} \|\boldsymbol{x} - \boldsymbol{x}^\star\|, \quad \forall \boldsymbol{x} \in \Omega, \tag{2}$$

where $\|\cdot\|$ denotes the Euclidean norm. The sign is different on the two sides of the interface and can be determined from sign $(\boldsymbol{n} \cdot (\boldsymbol{x} - \boldsymbol{x}^\star))$ with $\boldsymbol{x}^\star$ being the closest point on the interface to $\boldsymbol{x}$. A graphical representation of a the signed-distance function is given in Fig. 4(b).

For discretized domains, the values of the level-set function are typically stored at the nodes $\phi_i = \phi(\boldsymbol{x}_i)$, and the level-set function is interpolated by

$$\phi^h(\boldsymbol{x}) \quad = \quad \sum_{i \in I} N_i(\boldsymbol{x})\, \phi_i \tag{3}$$

using standard FE shape functions $N_i(\boldsymbol{x})$ as interpolation functions; I is the set of all nodes in Ω. The representation of the discontinuity as the zero-level of $\phi^h(\boldsymbol{x})$ is only an approximation of the real position, which improves with mesh refinement.

In some applications, the interface Γ_{12} moves throughout the simulation, i.e. $\phi(\boldsymbol{x})$ is also a function of time t (we still write $\phi(\boldsymbol{x})$ rather than $\phi(\boldsymbol{x}, t)$ for brevity). Then, the level-set function needs to be updated at each time-step. The most common approach for updating

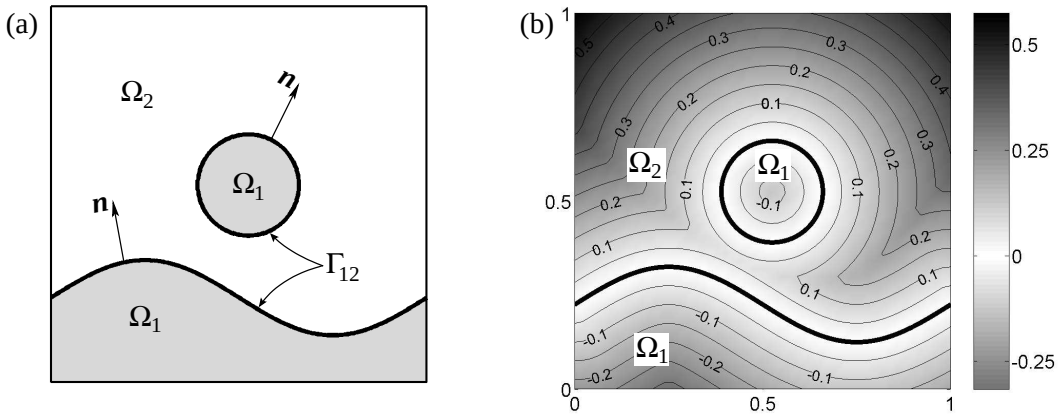

Figure 4. (a) The domain Ω decomposed into Ω_1 and Ω_2, (b) the signed-distance function for the description of the closed interfaces.

level-sets is to solve the equation

$$\frac{D\phi}{Dt} = 0 \quad \text{in } \Omega \times (0, t_{\text{end}})\,. \tag{4}$$

This can be rewritten as

$$\frac{\partial \phi}{\partial t} + \boldsymbol{u}\,(\boldsymbol{x}, t) \cdot \nabla \phi = 0 \quad \text{in } \Omega \times (0, t_{\text{end}})\,, \tag{5}$$

where $\boldsymbol{u}$ is a time-dependent velocity field with respect to the mesh. In many cases, only the velocity of the interface is known, and a velocity field is constructed by extension. The velocity is obtained from the physics of the underlying problem, e.g. the velocity of the crack front or the velocity of a phase interface. Equation (5) is a hyperbolic partial differential equation and stabilization is often needed for the solution [61]. It has been observed that using the same nodes for the approximation of (5) as for the underlying physical problem sometimes provides insufficient resolution for accurate updates of the level set function [177]. Then a refined set of nodes may be used for the level-set update.

Remarks

- It is well-known that due to the transport of the level-set function, the signed-distance property of (2) is lost. Furthermore, $\phi\,(\boldsymbol{x})$ tends to develop local high gradients over time. It is, therefore, often crucial to reinitialize the level-set function from time to time such that the signed-distance property is recovered, see e.g. [182, 154, 168]. This can also be done by means of the fast marching method, see e.g. [157, 158].
- Some authors suggest to solve (5) only locally near the interface rather than in the whole domain [143, 159]. Then, typically only a narrow region around the interface is considered.
- The area/volume of the two subdomains Ω_1 and Ω_2 is usually not conserved when a FE procedure is used for solving (5). The lack of conservation of certain quantities is intrinsic

in the FEM (and also XFEM). For this special application, however, the conservation may be enforced artificially e.g. by the approach proposed in [187].

- In closed domains without inflow and outflow boundaries, Dirichlet boundary conditions for the transport problem (5) are not needed. Otherwise, the prescription of values for the level-set function at the inflow boundaries may not be an easy task.

In the context of the XFEM, the level-set method for the description of fixed, closed interfaces has been proposed in Sukumar *et al.* [178] for material interfaces and holes. Moving closed interfaces in the XFEM are e.g. found in Chessa and Belytschko [47] and Fries [77] for two-phase flow problems and in Chessa *et al.* [50] for solidification problems. In Belytschko *et al.* [30, 31], the level-set method is not only used to describe internal interfaces but also to describe the domain boundaries on a background mesh.

3.2. Open interfaces

Cracks, dislocations, and shear bands are representatives of open interfaces, i.e. they (usually) end inside the domain Ω. Describing this by means of the level-set method requires an extension of the model as one level-set function is only able to define closed interfaces, see section 3.1. An extension of the level-set method for the description of cracks is given by Stolarska *et al.* [167, 166], which has also been used for shear bands e.g. by Areias and Belytschko [7]. A second level-set function $\gamma(\boldsymbol{x})$ is introduced which defines the position of the crack tip. The crack is then given by

$$\Gamma_c = \{\boldsymbol{x} : \ \phi(\boldsymbol{x}) = 0 \text{ and } \gamma(\boldsymbol{x}) \leq 0\}. \tag{6}$$

For a given crack geometry, it is suggested in [167, 166] to construct $\phi(\boldsymbol{x})$ and $\gamma(\boldsymbol{x})$ as follows: $\phi(\boldsymbol{x})$ is the signed-distance function which is zero on the crack surface and the tangential extension from the crack tip through the domain (i.e. $\phi(\boldsymbol{x})$ describes a closed interface). Then, $\gamma(\boldsymbol{x})$ is constructed such that it is orthogonal to Γ_c at the crack tip; $\gamma(\boldsymbol{x})$ is not necessarily a signed-distance function. The situation is sketched in Fig. 5 for a crack in a two-dimensional domain. Methods of branching and intersecting cracks with level-sets is described in [29].

When modeling crack propagation, the level-set functions ϕ and γ must be updated in each step. An effective procedure for these updates is described in [167, 166] for problems in two dimensions. In Moës *et al.* [127] and Gravouil *et al.* [91], non-planar crack growth problems in three dimensions are solved with the two level-set approach. A fast marching method for updating the level sets is proposed by Sukumar *et al.* [179] and Chopp and Sukumar [52] for planar cracks in three dimensions; for this case, one level-set suffices to describe the crack. An overview of different level-set approaches for the description and update of crack geometries is given by Duflot [68].

It is noted that the level-set method for crack propagation is somewhat different from the standard level-set method as described in section 3.1. This is due to the fact that crack propagation is an evolution of a surface *by a motion of its front* (generation of a new surface increment while the existing surface is fixed) rather than a moving interface completely described by a velocity field. This is the motivation for the description of the crack morphology by *vector* level-sets as proposed by Ventura *et al.* [192, 189] in the context of enriched methods and two-dimensional applications. The crack is defined by a vector level-set function which for each point $\boldsymbol{x} \in \Omega$ consists of the vector to the closest point $\boldsymbol{x}^\star$ on the crack surface

$$\tilde{\boldsymbol{\phi}}(\boldsymbol{x}) = \boldsymbol{x} - \boldsymbol{x}^\star \quad \forall \boldsymbol{x} \in \Omega, \tag{7}$$

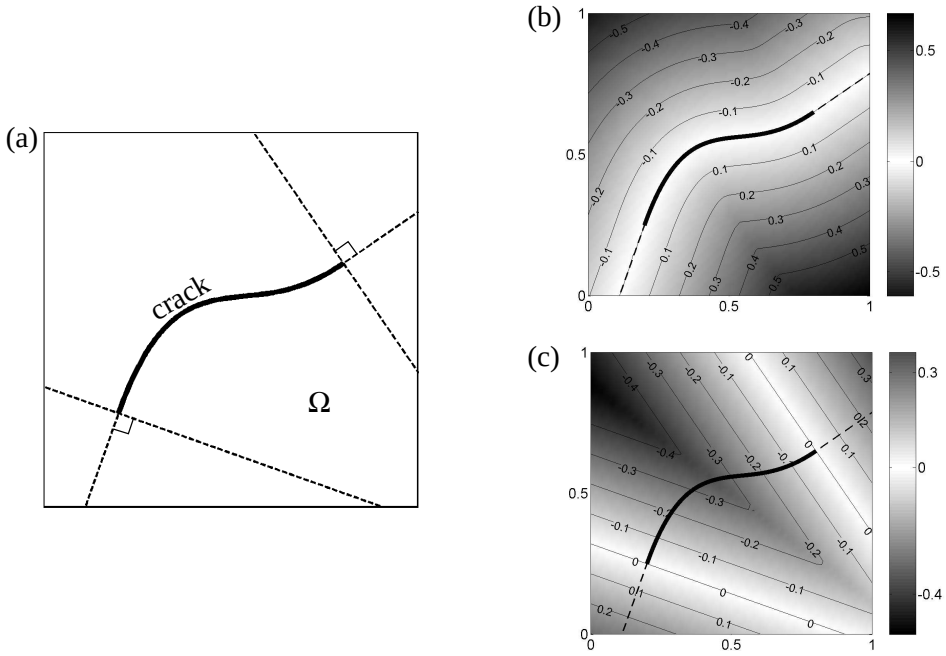

Figure 5. (a) The domain Ω with a crack, (b) the signed-distance function $\phi(\boldsymbol{x})$ for the description of the crack path, (c) the second level-set function $\gamma(\boldsymbol{x})$ for defining the crack tips.

and a sign-function $f(\boldsymbol{x})$ with opposite signs on the two sides of the crack. The crack geometry data is then a three-tuple in two dimensions and a four-tuple in three dimensions. The signed-distance function (2) is easily recovered as $\phi = \left\|\tilde{\boldsymbol{\phi}}(\boldsymbol{x})\right\| \cdot f(\boldsymbol{x})$. For a given crack increment, the update of the vector level-set does not require the solution of hyperbolic partial differential equations as e.g. (5), but simple geometric formulas are used [192, 189]. The existing crack surface remains fixed as desired, without any special treatment such as "freezing" the level-set function at certain nodes [91]. The vector level-set approach is used by Budyn *et al.* [38] for multiple interacting cracks in two dimensions.

4. Structure of the XFEM/GFEM

4.1. Global enrichment

Consider a d-dimensional domain $\Omega \in \mathbb{R}^d$ which is discretized by n^{el} elements, numbered from 1 to n^{el}. I is the set of all nodes in the domain, and I_k^{el} are the element nodes of element $k \in \left\{1, \ldots, n^{\text{el}}\right\}$. Our starting point is a finite element approximation of a function $u(\boldsymbol{x})$, $\boldsymbol{x} \in \Omega$, which is enriched *globally* [117, 16, 169], i.e. everywhere in Ω,

$$u^h(\boldsymbol{x}) = \underbrace{\sum_{i \in I} N_i(\boldsymbol{x})\, u_i}_{\text{strd. FE approx.}} + \underbrace{\sum_{i \in I} N_i^{\star}(\boldsymbol{x}) \cdot \psi(\boldsymbol{x})\, a_i}_{\text{enrichment}}, \tag{8}$$

where, for simplicity, only one enrichment term is considered. It can clearly be seen that the standard FE approximation is extended by the (extrinsic) enrichment term. In (8), N_i and $N_i^\star$ are standard FE shape functions, which are often but not necessarily chosen identical (however, $N_i^\star = N_i$ is assumed in the following unless mentioned otherwise). The coefficients u_i belong to the standard FE part and a_i are additional nodal unknowns. The function $\psi(\boldsymbol{x})$, as indicated above, is called an *enrichment function* and it is this function which incorporates the special knowledge about a solution (e.g. jumps, kinks, singularities etc.) into the approximation space. The products $N_i^\star(\boldsymbol{x}) \cdot \psi(\boldsymbol{x})$ may be termed *local* enrichment functions because their supports coincide with the supports of typical FE shape functions, leading to sparsity in the discrete equations. We note that the definition of the approximation $u^h(\boldsymbol{x})$ as given in the partition of unity method [16] (or equally in the partition of unity finite element method [117] or particle-partition of unity method [92, 93]) is more general than (8), because N_i, $N_i^\star$ can then be any functions that build a partition of unity, i.e. also meshfree functions.

The structure of the enrichment term plays a crucial role in the PUM, GFEM, and XFEM: The functions $N_i^\star$ build a partition of unity over the domain, i.e. Ω,

$$\sum_{i \in I} N_i^\star(\boldsymbol{x}) = 1. \tag{9}$$

As a consequence, it can be shown that the approximation (8) can reproduce *any* enrichment function exactly in Ω, see Melenk and Babuška [117, 16]. Therefore, it is often said that the enrichment is realized through the partition of unity concept. The special structure of the enrichment differentiates the PUM, GFEM, and XFEM from other methods which add terms to the standard FE approximation such as for example the global-local FEM [130, 134] or the discontinuous enrichment method [39, 72, 99]. Theoretical investigations that give insight on how the enrichment works in the partition of unity context are found in Babuška *et al.* [12, 13] and Schweitzer [156].

Approximations of the form (8) do not, in general, have the Kronecker-δ property. Consequently, $u^h(\boldsymbol{x}_i) \neq u_i$ which renders the imposition of essential boundary conditions difficult. Furthermore, the interpretation of the results is more difficult as $u^h(\boldsymbol{x}_i)$ has to be constructed correctly by evaluating all terms in the approximation. It is, therefore, desirable to have enrichment terms that vanish at all nodes, thereby recovering the Kronecker-δ property of standard FE approximations. This is achieved by *shifting* the approximation as

$$u^h(\boldsymbol{x}) = \sum_{i \in I} N_i(\boldsymbol{x})\, u_i + \sum_{i \in I} N_i^\star(\boldsymbol{x}) \cdot [\psi(\boldsymbol{x}) - \psi(\boldsymbol{x}_i)]\, a_i, \tag{10}$$

which was first suggested in [29]. It can be shown that this formulation is still able to reproduce the enrichment function $\psi(\boldsymbol{x})$ exactly.

It is important to note that while (10) has the Kronecker-δ property, the enrichment terms may still be non-zero on parts of the element boundary between the nodes. This may influence the imposition of essential boundary conditions as discussed in section 9. In the following, we often write approximations in their un-shifted form for brevity. For implementations, shifted approximations are recommended.

4.2. Local enrichment

A global enrichment as in (8) and (10) is computationally demanding because the number of enriched degrees of freedom is proportional to the number of nodes in Ω. The approximation

of discontinuities and high gradients, as discussed in section 2, involves *local* phenomena and it is clearly not efficient to enrich globally. Typically, the enrichment is localized by reducing the number of enriched nodes, i.e. enriching nodes in a subset $I^\star \subset I$. This leads to an approximation of the form

$$u^h(\boldsymbol{x}) = \sum_{i\in I} N_i(\boldsymbol{x})\, u_i + \sum_{i\in I^\star} N_i^\star(\boldsymbol{x}) \cdot [\psi(\boldsymbol{x}) - \psi(\boldsymbol{x}_i)]\, a_i, \tag{11}$$

which is a standard XFEM approximation.

Because only a subset of the nodes is enriched, each element falls into one of the following categories: The element is (i) a standard finite element if *none* of the element nodes are enriched, (ii) a reproducing elements if *all* element nodes are enriched, or (iii) a blending element if *some* of the element nodes are enriched, see Fig. 6(a) and (c). An important observation is that the functions $N_i^\star(\boldsymbol{x})$ only build a partition of unity over the *reproducing* elements, see Fig. 6(b) and (d). Only in these elements, the enrichment function can be reproduced exactly.

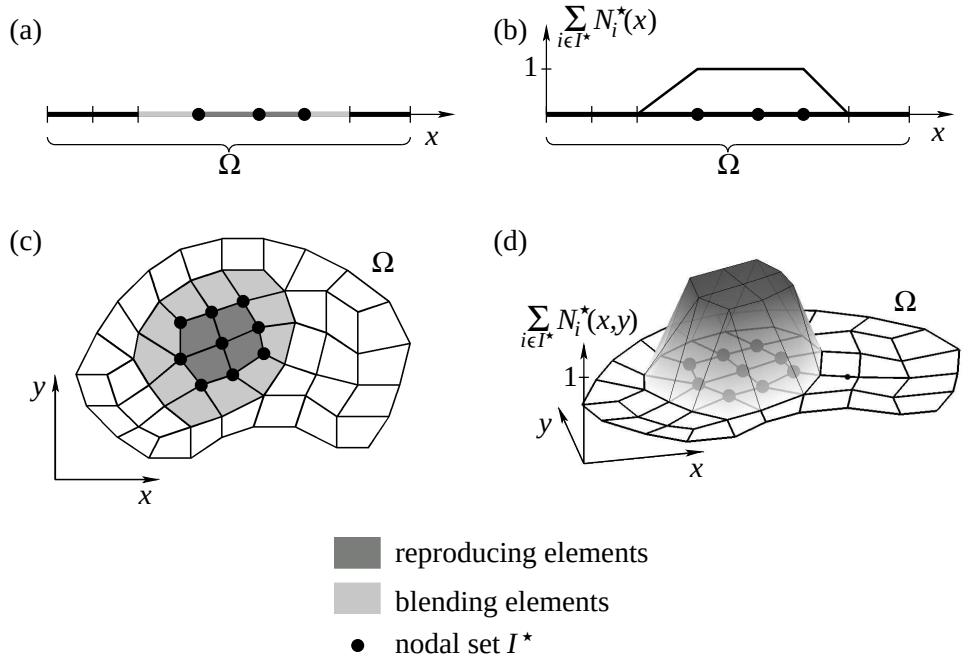

Figure 6. Discretized domains in one and two dimensions with nodal subset $I^\star$. (a) and (c) show the reproducing and blending elements as a consequence of the choice of $I^\star$. (b) and (d) show that the functions $N_i^\star(\boldsymbol{x})$ are a partition of unity in the reproducing elements, but $\sum_{i\in I^\star} N_i^\star(\boldsymbol{x}) \neq 1$ in the blending elements.

It is, in particular, noteworthy to consider the situation in the blending elements. There, the functions $N_i^\star(\boldsymbol{x})$ are non-zero but they do not build a partition of unity. A consequence is that (i) the enrichment function cannot be reproduced exactly, and (ii), more troublesome, additional, parasitic terms are added to the approximation. This is discussed by Chessa *et*

al. [51], Fries [76], Gracie *et al.* [90], and Ventura *et al.* [190]. Herein, we only give one example of the pathology: Consider the situation where only *one* node of a blending element is enriched by some non-polynomial enrichment. Then, when the corresponding unknown is non-zero, there are terms which can not be compensated by the standard polynomial-based FE part of the approximation.

It is important to note that while parasitic terms are present in blending elements for general enrichment functions; they do *not* occur for enrichment functions which are zero or constant in the blending elements. The convergence rates of XFEM approximations may be drastically reduced by the parasitic terms in the blending elements, see e.g. [178, 51, 76, 90]. However, the influence of the parasitic terms is not easily predicted: For some enrichments they may reduce the convergence rate (e.g. for the abs-enrichment, see section 5.1.3), for others they may only increase the absolute error while keeping the convergence rate unchanged (e.g. for crack tip enrichments, see section 5.2.2) [76]. Different strategies for overcoming these problems are discussed in the next subsection. We note that blending elements are not discussed in the GFEM literature as often global enrichments are used. In contrast, the localization of the enrichment by enriching a subset of the nodes in the domain ($I^\star$) has been an important part of the XFEM from the beginning.

We end this subsection by mentioning that sometimes it is desirable to cluster some of the enriched nodes in (11), and constrain the enrichment parameters at these nodes to be equal, see e.g. Laborde *et al.* [108] and Ventura *et al.* [190]. Let the nodes in $I^\star$ be divided into k non-overlapping sets $I_1^\star, \ldots, I_k^\star$, then a clustered approximation is

$$u^h(\boldsymbol{x}) = \sum_{i\in I} N_i(\boldsymbol{x})\, u_i + \sum_{j=1}^{k} \Big(\sum_{i\in I_j^\star} N_i^\star(\boldsymbol{x}) \Big) \cdot \psi(\boldsymbol{x})\, a_j. \tag{12}$$

Consequently, there are only k additional unknowns for a scalar function. The band-width, on the other hand, increases. This is known as a *flat-top* enrichment, see Fig. 7. This approach has also been called degrees-of-freedom-gathering XFEM in Laborde *et al.* [108]. These approaches are particularly useful if the conditioning of the system matrix is prohibitively bad when all nodes in $I^\star$ are enriched.

4.3. Blending elements

Difficulties in blending elements have already been reported in early XFEM publications such as [178, 51]. Again, it is noted that for piecewise constant enrichment functions, there are no difficulties in blending elements. We classify four approaches for remedying unsatisfactory behavior in blending elements. These remedies have all been able to achieve optimal convergence rates for cases where the standard XFEM approximation (11) could not. However, they differ significantly in their applicability to general models, enrichments and element types.

Corrected or weighted XFEM. In Fries [76], a global enrichment function is localized through the multiplication by a ramp function $R(\boldsymbol{x})$. Then, all nodes of the domain where this localized enrichment function is non-zero are enriched. Consequently, the enrichment vanishes in those elements where only some of the nodes are enriched and no difficulties occure in blending elements. The approximation becomes

$$u^h(\boldsymbol{x}) = \sum_{i\in I} N_i(\boldsymbol{x})\, u_i + \sum_{i\in I^\star} N_i^\star(\boldsymbol{x}) \cdot R(\boldsymbol{x}) \cdot [\psi(\boldsymbol{x}) - \psi(\boldsymbol{x}_i)]\, a_i, \tag{13}$$

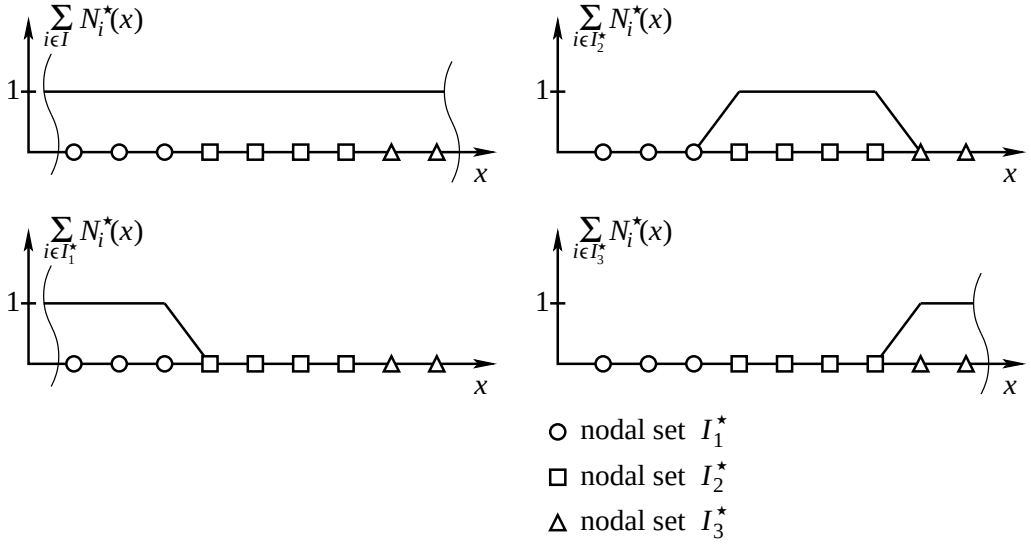

Figure 7. The figure shows a part of an enriched one-dimensional domain discretized by linear finite elements. The degrees of freedom at the nodes are clustered such that only one enrichment degree of freedom results for all the nodes in each $I_i^\star$, $i = 1, 2, 3$. The partition of unity is built by these flat-top functions.

where $R(\boldsymbol{x})$ is constructed by means of FE shape functions; an example may be seen in Fig. 6(b) and (d). This approach is called "corrected XFEM". It is simple and general, and it does not lead to additional terms in the weak form. Later, in Chahine *et al.* [43], a similar approach was used for crack tip enrichments, where the ramp function is called a cutoff function. The corrected XFEM was further discussed and investigated in Ventura *et al.* [190] where the authors call the ramp function "weight function" and use the term "weighted XFEM". Instead of using the product $R(\boldsymbol{x}) \cdot [\psi(\boldsymbol{x}) - \psi(\boldsymbol{x}_i)]$ in order to achieve a (guaranteed) smooth transition in the blending elements, one may sometimes use only a ramp function $R(\boldsymbol{x})$ in the blending elements as long as the required continuity properties are fulfilled. The latter approach is justified by the fact that we can not reproduce the enrichment function in the blending elements anyway.

Suppressing blending elements by coupling enriched and standard regions. In this approach, the domain is decomposed into a region where all nodes are enriched and a standard FE region without enrichment. Then, no blending elements exist, see Fig. 8. The two regions are coupled by enforcing continuity. The coupling has been realized point-wise at nodes in Laborde *et al.* [108], and although the continuity along the element edges is not ensured, remarkably good results are obtained. In Gracie *et al.* [90], the coupling is realized by a discontinuous Galerkin method based on interior penalty terms. Then, additional terms in the weak form have to be evaluated. The use of other standard methods for enforcing additional constraints such as Lagrange multipliers (e.g. the mortar method), penalty method, or Nitsche's method for the continuity along the interface between enriched and standard elements is also an alternative (though results are not yet reported).

Hierarchical shape functions in blending elements. Hierarchical shape functions in

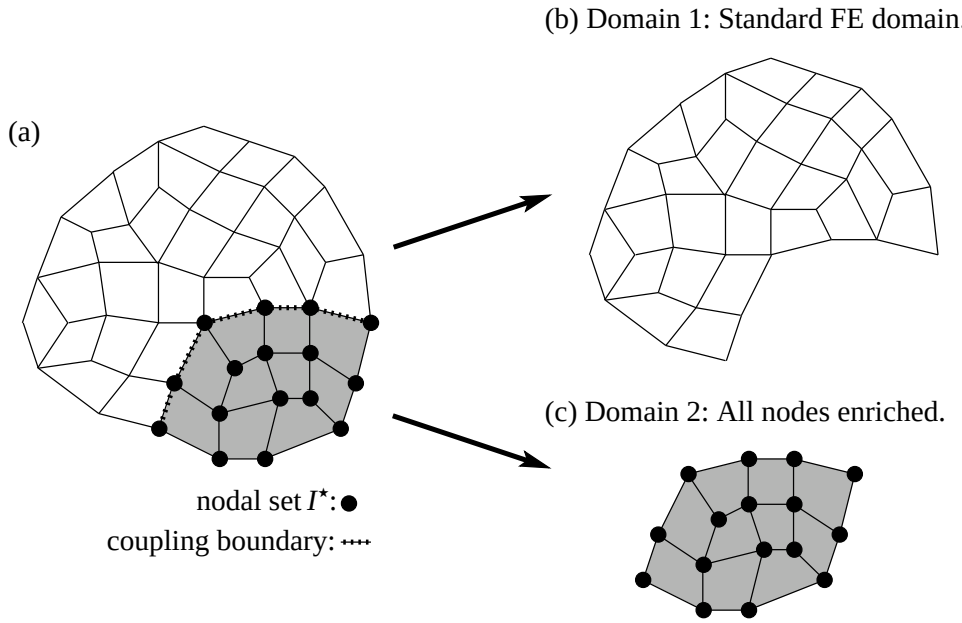

Figure 8. Suppressing blending elements by decomposing the domain into two subdomains: (b) a standard finite element domain and (c) a fully enriched domain. The continuity along the shared boundaries is enforced lateron.

the blending elements may be added to the standard FE part of the approximation in order to compensate for the parasitic terms. Consequently, this approach increases the number of degrees of freedom. It has was used in Chessa *et al.* [51] for linear, triangular elements, and has recently been extended to higher-order elements by Tarancón *et al.* [185]; however, the results are not always optimal.

Assumed strain blending elements. Special enhanced strain elements have been proposed with the aim to cancel out the parasitic terms. This requires the incorporation of the exact form of the parasitic terms in the blending elements, and they are element and enrichment dependent. Linear assumed strain blending elements for weak discontinuities are proposed in Chessa *et al.* [51] and for crack tip enrichments in Gracie *et al.* [90]. The adjustment of this approach for different elements and enrichments is quite involved.

4.4. Extension to several enrichments and vector fields

Now we give the aforementioned XFEM approximation (11) for the case of several enrichments and vector fields. The resulting formulations extend in a straightforward way also to the case of un-shifted global enrichments (8), shifted global enrichments (10), clustered enrichments (12), and corrected XFEM enrichments (13).

Several enrichments. In many applications of the XFEM, several enrichments shall be

added. For m enrichment terms, the approximation becomes

$$u^h(\boldsymbol{x}) = \sum_{i\in I} N_i(\boldsymbol{x})\, u_i + \sum_{j=1}^{m} \sum_{i\in I_j^\star} N_i^\star(\boldsymbol{x}) \cdot \left[\psi^j(\boldsymbol{x}) - \psi^j(\boldsymbol{x}_i)\right] a_i^j \tag{14}$$

where $I_j^\star$ and ψ^j are the nodal subsets of enriched nodes and corresponding enrichment functions, respectively. When using several enrichments, special care is sometimes required in order to ensure that the resulting approximation space is still linearly independent.

Enrichment of vector fields. Often, vector fields such as displacement or velocity fields have the same attributes across an interface. For example, cracks lead to a jump in each of the displacement components, whereas kinks are present in each of the velocity components at interfaces in two-phase flows. Then, the approximations of the d components $\boldsymbol{u}(\boldsymbol{x}) = [u(\boldsymbol{x}), v(\boldsymbol{x}), \dots]$ of the vector field are enriched as

$$\boldsymbol{u}^h(\boldsymbol{x}) = \sum_{i\in I} \boldsymbol{N}_i(\boldsymbol{x})\, \boldsymbol{u}_i + \sum_{i\in I^\star} \boldsymbol{N}_i^\star(\boldsymbol{x}) \cdot [\psi(\boldsymbol{x}) - \psi(\boldsymbol{x}_i)]\, \boldsymbol{a}_i. \tag{15}$$

Herein, $\boldsymbol{u}_i = [u_i, v_i, \dots]$ and $\boldsymbol{a}_i = [a_i, b_i, \dots]$ are the unknowns of the components of the vector field.

Enrichment of tangential components of vector fields. Sometimes, the special solution properties of a vector field only take place tangent to the interface. This is for example the case for dislocations and shear band models where the jump occurs in the tangential displacement at the interface. Then, a tangential enrichment of the following form is appropriate in two dimensions [29],

$$\boldsymbol{u}^h(\boldsymbol{x}) = \sum_{i\in I} \boldsymbol{N}_i(\boldsymbol{x})\, \boldsymbol{u}_i + \sum_{i\in I^\star} \boldsymbol{N}_i^\star(\boldsymbol{x}) \cdot \boldsymbol{t}\ [\psi(\boldsymbol{x}) - \psi(\boldsymbol{x}_i)]\, a_i, \tag{16}$$

where $\boldsymbol{t} \in \mathbb{R}^d$ is the unit tangent vector along the interface. In contrast to the situation where all components are discontinuous, only *one* set of XFEM unknowns a_i is needed. In three dimensions, two tangent vectors $\boldsymbol{t}_1$ and $\boldsymbol{t}_2$ and two sets of XFEM unknowns a_i and b_i are needed.

5. Enrichments and applications

In the previous section, the general formulation of enriched approximations has been given. A particular realization of these approximations is characterized by the choice of the enriched nodes and the corresponding enrichment functions. Here, according to the phenomena discussed in section 2, we distinguish between enrichment functions for (i) discontinuities across closed interfaces, (ii) discontinuities across open interfaces (as they appear in e.g. in cracks) and (iii) high-gradients. For each of these phenomena, the corresponding enrichment schemes are given together with an overview of related applications.

5.1. Discontinuities across closed interfaces

The modeling of closed interfaces by level-sets has been discussed in section 3.1. *Strong* discontinuities across closed interfaces are e.g. found in the stress and strain fields of bi-material structures, or in the pressure fields of incompressible two-phase flows with surface

tension. *Weak* discontinuities at closed interfaces appear frequently in solutions of multi-material applications (i.e. where material properties jump across interfaces). They are found for example in the displacement fields of bi-material structures, or in the velocity fields of two-phase flows.

5.1.1. Enriched nodes Assume that the position of the closed interface is given implicitly by the level-set function $\phi(\boldsymbol{x})$ as discussed in section 3.1. All nodes of elements cut by the interface are enriched, see Fig. 9. Whether or not an element is cut by the discontinuity can conveniently be determined on the element-level by means of the level-set function. The set of cut elements is

$$\mathcal{N}_\phi = \Big\{ k \in \big\{1, \dots, n^{\mathrm{el}}\big\} : \min_{i \in I_k^{\mathrm{el}}} \left(\phi(\boldsymbol{x}_i)\right) \cdot \max_{i \in I_k^{\mathrm{el}}} \left(\phi(\boldsymbol{x}_i)\right) < 0 \Big\}, \tag{17}$$

where I_k^{el} are the element nodes of element k. The set of enriched nodes $I_\phi^\star$ follows from (17) as

$$I_\phi^\star = \bigcup_{k \in \mathcal{N}_\phi} I_k^{\mathrm{el}}. \tag{18}$$

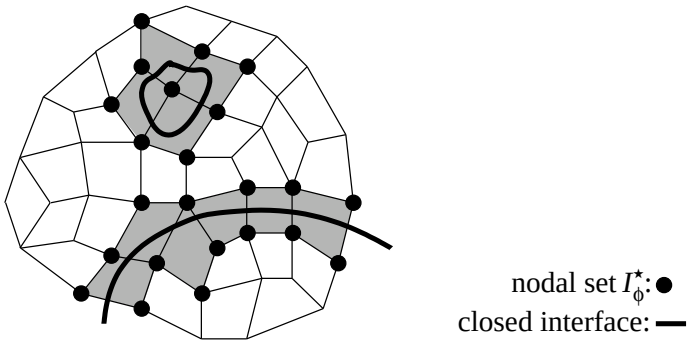

Figure 9. Nodal set of enriched nodes $I_\phi^\star$ for closed interfaces.

5.1.2. Enrichment functions for strong discontinuities A typical choice of the enrichment function $\psi(\boldsymbol{x})$ in the presence of strong discontinuities is the sign of the level-set function,

$$\psi_{\mathrm{sign}}(\boldsymbol{x}) = \mathrm{sign}\left(\phi(\boldsymbol{x})\right) = \begin{cases} -1 & : \phi(\boldsymbol{x}) < 0, \\ 0 & : \phi(\boldsymbol{x}) = 0, \\ 1 & : \phi(\boldsymbol{x}) > 0. \end{cases} \tag{19}$$

Also the Heaviside function

$$\psi_{\mathrm{H}}(\boldsymbol{x}) = \mathrm{H}\left(\phi(\boldsymbol{x})\right) = \begin{cases} 0 & : \phi(\boldsymbol{x}) \leq 0, \\ 1 & : \phi(\boldsymbol{x}) > 0, \end{cases} \tag{20}$$

may be chosen. The sign and Heaviside enrichments lead to identical results as they span the same approximation space. Therefore, in the rest of this paper, the general expression "step-enrichment" refers to either the sign or Heaviside enrichment, i.e.

$$\psi_{\mathrm{step}} = \psi_{\mathrm{sign}} \qquad \text{or} \qquad \psi_{\mathrm{step}} = \psi_{\mathrm{H}}. \tag{21}$$

These enrichments have been proposed in some of the earliest studies of the XFEM such as by Belytschko and Black [23], Moës *et al.* [126], and Sukumar *et al.* [180].

It is important to note that shifted step enrichments vanish outside the elements crossed by the discontinuities, so only these elements need to be modified; essentially there are no blending elements. Even for un-shifted step enrichments, blending causes no difficulties because the enrichments are constant in the blending elements. However, in contrast to shifted step enrichments, the blending elements differ from standard finite elements, since the enrichment is nonzero in these elements.

Hansbo and Hansbo [97] have developed an innovative method for modeling discontinuities where the approximation is constructed from two fields, u_1 and u_2. If an interface is described by the level-set function $\phi(\boldsymbol{x})$ and cuts the domain completely in two, the approximation can then be written as

$$u^h(\boldsymbol{x}) = u_1^h(\boldsymbol{x}) \cdot \mathrm{H}(\phi(\boldsymbol{x})) + u_2^h(\boldsymbol{x}) \cdot \mathrm{H}(-\phi(\boldsymbol{x})). \tag{22}$$

This approximation naturally introduces a strong discontinuity along the interface, i.e. at $\phi(\boldsymbol{x}) = 0$. In the implementation, this dual field is only constructed for the elements that are cut by the discontinuity, so the implementation is straightforward. It is shown in Areias and Belytschko [6] that the Hansbo and Hansbo basis functions are identical to those of the shifted step-enrichment in the XFEM.

5.1.3. Enrichment functions for weak discontinuities For weak discontinuities, one choice (and the earliest) for the enrichment function at the nodes $I_\phi^\star$ is the absolute value of the level-set function [29, 178],

$$\psi_{\mathrm{abs}}(\boldsymbol{x}) = \mathrm{abs}(\phi(\boldsymbol{x})) = |\phi(\boldsymbol{x})|, \tag{23}$$

which was first used in a meshfree context in [106]. The gradient is given by

$$\nabla\psi_{\mathrm{abs}}(\boldsymbol{x}) = \mathrm{sign}(\phi(\boldsymbol{x})) \cdot \nabla\phi(\boldsymbol{x}). \tag{24}$$

This enrichment function leads to well-known problems in blending elements. In the context of a standard XFEM approximation (11), it leads to sub-optimal results, so the remedies discussed in section 4.3 are recommended.

An interesting alternative for weak discontinuities is the following enrichment

$$\psi_{\mathrm{abs}}(\boldsymbol{x}) = \sum_{i\in I} |\phi_i| N_i(\boldsymbol{x}) - \Big| \sum_{i\in I} \phi_i N_i(\boldsymbol{x}) \Big|, \tag{25}$$

which was proposed by Moës *et al.* [125]. This enrichment vanishes outside of the elements crossed by the weak discontinuity, so just as for the shifted step enrichment, there is no need for special treatment of the blending elements.

A third alternative is to use enrichments for *strong* discontinuities and then enforce continuity as first proposed by Hansbo and Hansbo [96]; a weak discontinuity then results. They used Nitsche's method to enforce continuity. Lagrange multipliers, as in Zilian and Legay [207], can also be used for the continuity constraint. Dolbow and Harari [56], have generalized this approach for combined strong and weak discontinuities as further discussed later.

5.1.4. Applications in solid mechanics Applications of the XFEM for closed interfaces in solids are found e.g. for inclusions, holes, topology optimization, and grain boundaries. Cracks and dislocations involve open interfaces and are discussed in section 5.2. The XFEM has been applied for *inclusions* in solids by Sukumar *et al.* [178]. The abs-enrichment is used in order to capture the weak discontinuities in the displacement fields at the material interfaces. However, due to problems in blending elements, only sub-optimal results are achieved in [178]. Optimal convergence rates for material interfaces were later obtained e.g. by Chessa *et al.* [51], Moës *et al.* [125], and Fries [76].

Holes in solids were considered in the framework of the XFEM using the step enrichment by Sukumar *et al.* [178]. It is noted that holes and voids may also be treated within a classical FEM framework, i.e. without enrichments: The element areas inside the hole are simply neglected in the integration of the weak form. In a similar application the boundaries of a domain were defined implicitly by level sets with a Cartesian background mesh; the part outside the domain is then the "hole". This approach has been employed for *topology optimization* with XFEM by Belytschko *et al.* [31].

Grain boundaries are modeled with the XFEM by Simone *et al.* [162]. Applications of the XFEM in the field of *phase transitions* and *solidification* are found by Chessa *et al.* [50], Ji *et al.* [102], and Merle and Dolbow [121]. *Bio-mechanical* applications with closed interfaces are found e.g. in Duddu *et al.* [67] and Smith *et al.* [163]. As reported by Jeřábková and Kuhlen [101] and Vigneron *et al.* [193], the XFEM can also be used successfully for the modeling of virtual cuts within *surgical simulators*.

5.1.5. Applications in fluid mechanics In fluid mechanics, the XFEM has been applied for two-phase flows and fluid-structure interaction. Immiscible *two-phase flows* are examples where a moving interface separates two different fluids (liquids or gases). The velocity fields are weakly discontinuous across the interface. The pressure field may be strongly discontinuous if surface tension effects are considered, otherwise, it is weakly discontinuous. Surface tension effects depend on the curvature of the fluid-fluid interface and we refer the interested reader to [95, 77] for how this can be handled in the context of the level-set method. The XFEM has first been used for two-phase flows by Chessa and Belytschko [47, 46]. They use a fractional step method to uncouple the momentum and continuity equation. Only the velocity fields are enriched by the abs-enrichment. Groß and Reusken [95] use step-enriched pressure fields for two-phase flows with surface tension. The velocity fields are not enriched but the mesh is refined near the interface. The intrinsic XFEM is used in Fries [77] for two-phase flows with surface tension. The velocity *and* pressure fields are enriched accordingly.

In most *fluid-structure interaction* (FSI) problems that have been modeled by the XFEM, the fluid-structure interface Γ_{FS} is described by the level-set method. Depending on whether slip or no-slip conditions are assumed along the fluid-structure interface, the tangential velocity field at Γ_{FS} may be strongly or weakly discontinuous, respectively. Applications of the XFEM for moderately complex structures interacting with a flow are found in Legay *et al.* [111], Gerstenberger and Wall [84], and Wagner *et al.* [194]. Degenerated structures are realized by Legay and Tralli [112] and Zilian and Legay [207]. Gerstenberger and Wall [83] use conforming meshes in the vicinity of the structure and couple this local fluid-structure region with a background fluid domain.

5.2. Discontinuities across open interfaces

Many applications involve discontinuities along interfaces that end inside the domain, i.e. the interface has a tip in two spatial dimensions or a front in three dimensions. Moreover, in many physics problems, high gradients are present in the field variables at the interface tip or front. Thus, for the simulation of such problems, both the discontinuities along the interface *and* the high gradients at the interface tip/front must be considered appropriately. In the XFEM, this is typically achieved by using a different enrichment scheme for each of these two features.

Cracks and dislocations are examples where the displacement fields involve jumps across open interfaces and have high gradients at the crack tips or dislocation cores, respectively. Shear bands when modeled with zero width have a tangential jump across open interfaces. Cracks are a particularly important topic in the XFEM as most applications of this method so far have been realized in this field and they are of great engineering relevance.

In contrast to the situation described in section 5.1 for strong and weak discontinuities at closed interfaces—where the step and abs-enrichment apply for a large number of applications—the enrichment functions employed at interface tips/fronts depend on the particular physical model under consideration. Therefore, in the following the enrichment functions are discussed with respect to particular applications.

5.2.1. Enriched nodes Two sets of nodes are defined which are enriched differently. The enrichments for the high gradients at the interface tip/front are realized at the nodes in

$$I^{\star}_{\text{tip}} = \left\{ \boldsymbol{x} : \left\| \boldsymbol{x} - \boldsymbol{x}^{\star}_{\text{tip}} \right\| \leq r \right\}, \tag{26}$$

where $\boldsymbol{x}^{\star}_{\text{tip}}$ is the interface tip in two dimensions or the nearest point on the interface front in three dimensions and $r \in \mathbb{R}$ is a prescribed radius [108, 22], see Fig. 10(a). Rather than using this geometric criterion, it is sometimes useful to enrich only the element nodes of the elements containing the interface tip/front [126], see Fig. 10(b). Assume that these elements are given in the set $\mathcal{M}$, then

$$I^{\star}_{\text{tip}} = \bigcup_{k \in \mathcal{M}} I^{\text{el}}_{k}. \tag{27}$$

Nodes along the interface are enriched differently and are in

$$I^{\star}_{\phi,\gamma} = \left\{ \bigcup_{k \in \mathcal{N}_{\phi,\gamma}} I^{\text{el}}_{k} \right\} \setminus I^{\star}_{\text{tip}}. \tag{28}$$

where $\mathcal{N}_{\phi,\gamma}$ is the set of elements that are completely cut by the open interface,

$$\mathcal{N}_{\phi,\gamma} = \left\{ k \in \left\{1, \ldots, n^{\text{el}}\right\} : \min_{i \in I^{\text{el}}_{k}} \left(\phi\left(\boldsymbol{x}_i\right)\right) \cdot \max_{i \in I^{\text{el}}_{k}} \left(\phi\left(\boldsymbol{x}_i\right)\right) < 0 \text{ and } \max_{i \in I^{\text{el}}_{k}} \left(\gamma\left(\boldsymbol{x}_i\right)\right) < 0 \right\}. \tag{29}$$

The two level-set functions $\phi\left(\boldsymbol{x}\right)$ and $\gamma\left(\boldsymbol{x}\right)$ define the open interface as discussed in section 3.2. A graphical representation of the two nodal sets $I^{\star}_{\text{tip}}$ and $I^{\star}_{\phi,\gamma}$ is given in Fig. 10.

5.2.2. Enrichment functions for brittle cracks We first consider cracks in brittle materials in the framework of linear elastic fracture mechanics. In that case, the stresses and strain fields at the crack tip are *singular*. The following four enrichment functions $\psi^{1}_{\text{tip}}\left(\boldsymbol{x}\right)$ to $\psi^{4}_{\text{tip}}\left(\boldsymbol{x}\right)$ are based on the asymptotic solution of Williams [198]

$$\boldsymbol{\psi}_{\text{tip}}\left(\boldsymbol{x}\right) = \left\{ \sqrt{r} \sin\frac{\theta}{2},\ \sqrt{r} \sin\frac{\theta}{2} \sin\theta,\ \sqrt{r} \cos\frac{\theta}{2},\ \sqrt{r} \cos\frac{\theta}{2} \sin\theta \right\}, \tag{30}$$

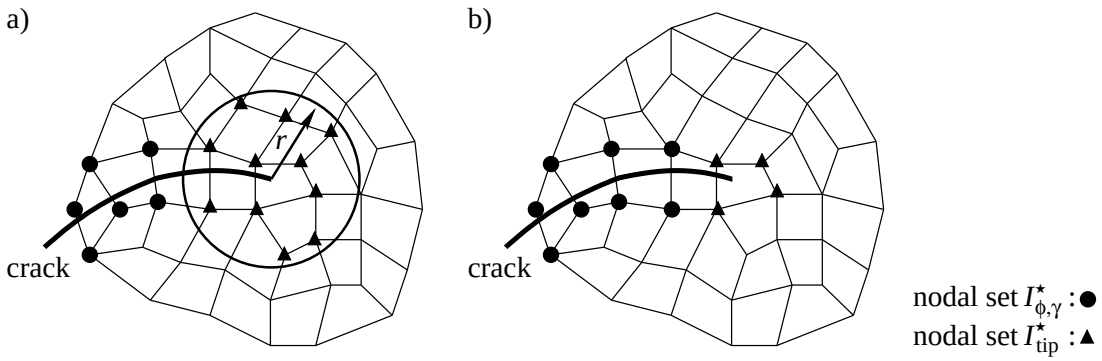

Figure 10. Enriched nodal sets for open interfaces (e.g. cracks and dislocations). Near the interface front (crack tip or dislocation core), different enrichments are used at the nodes in $I^{\star}_{\text{tip}}$ than along the interface at the nodes in $I^{\star}_{\phi,\gamma}$.

and span the first order terms in that asymptotic solution for mode I and mode II loadings of cracks; they were introduced in meshfree methods by Fleming *et al.* [75]. They are found in the first applications of the XFEM in Belytschko and Black [23] and Moës *et al.* [126]. These functions depend on a local coordinate system (r, θ) at the crack tip, see Fig. 11. Expressing the enrichment in terms of two level-set functions $\phi(\boldsymbol{x})$ and $\gamma(\boldsymbol{x})$ as described in section 3.2 enables the enrichment to model curved cracks, see e.g. [29, 167]. A graphical representation of (30) may be found in Fig. 12. It is noted that these enrichment functions are used for the displacement fields and have a singularity in their *derivatives* (because the stresses and strains are singular, not the displacements).

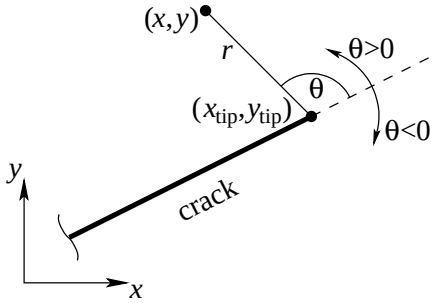

Figure 11. Coordinate system (r, θ) at a crack tip.

Belytschko and Black [23] use the enrichment functions (30) for the complete crack path and treat kinks in the crack path by special mappings, as previously suggested in [75] in a meshfree context. The combination of these enrichments near the crack tip and the use of the step enrichment along the crack path was suggested in Moës *et al.* [126] and has developed to be a standard in XFEM: Let $\boldsymbol{u}^h(\boldsymbol{x})$ be the XFEM approximations of the components of the

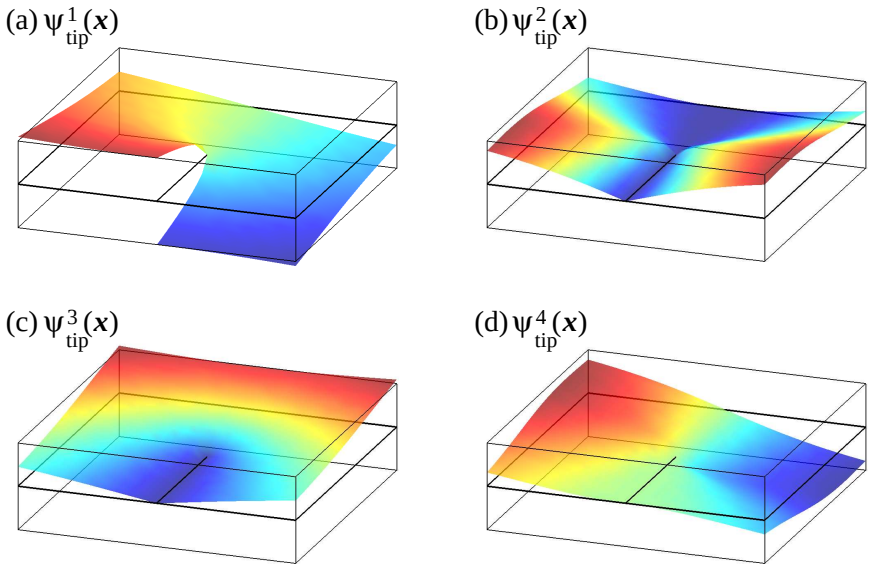

Figure 12. Enrichment functions $\psi^i_{\text{tip}}(\boldsymbol{x})$, $i = 1, 2, 3, 4$, for a crack tip enrichment for brittle materials in the frame of linear elastic fracture mechanics.

displacement field, then

$$\boldsymbol{u}^h(\boldsymbol{x}) = \sum_{i\in I} \boldsymbol{N}_i(\boldsymbol{x})\,\boldsymbol{u}_i + \sum_{i\in I^\star_{\phi,\gamma}} \boldsymbol{N}^\star_i(\boldsymbol{x})\,\psi_{\text{step}}(\boldsymbol{x})\,\boldsymbol{a}_i + \tag{31}$$

$$\sum_{j=1}^{4}\sum_{i\in I^\star_{\text{tip}}} \boldsymbol{N}^\star_i(\boldsymbol{x})\,\psi^j_{\text{tip}}(\boldsymbol{x})\,\boldsymbol{b}^j_i, \tag{32}$$

which is given in the un-shifted form for brevity. The second enrichment term is used at the complete crack front: In two-dimensions, it is employed at each crack tip (*one* for edge cracks, *two* for cracks that are completely inside the domain). In three dimensions, the same crack tip enrichment is often used along the crack front with θ being the angle to the tangent plane at the front [180]. The justification for using the same enrichment functions (30) in three dimensions is that the asymptotic fields near the crack front are two-dimensional in nature, except near surfaces. The first application of XFEM to three-dimensional crack problems is by Sukumar *et al.* [180, 179]; subsequent developments can be found in Moës *et al.* [127], Gravouil *et al.* [91], Areias and Belytschko [5]; application of GFEM to three dimensional cracks is found in Duarte *et al.* [63].

We give a brief overview of extensions of the XFEM for cracks. Surveys with more details on the application of XFEM in fracture mechanics can be found by Belytschko *et al.* [26], Karihaloo and Xiao [104], and Mohammadi [128].

- The approximation for several cracks is achieved in a straightforward manner by adding the crack path and crack tip enrichment individually for each crack.
- For branching and intersection cracks, the use of the step enrichment of section 5.1.2 is no longer sufficient. Daux *et al.* [55] introduce a step enrichment function for crack junctions which does not rely on level-sets. The enrichment for intersecting and branching cracks based on level-sets is given by Belytschko *et al.* [29].
- Karihaloo, Xiao and co-workers [115, 199, 201] include higher order terms of the asymptotic expansion of the crack tip field as enrichment functions. One degree of freedom is associated with each enrichment function in the sense of a flat-top enrichment, see section 4.2. As a consequence, the stress intensity factors are directly obtained rather than through a post-processing step.
- Special crack tip enrichments for orthotropic media are given by Asadpoure and Mohammadi [9] and Mohammadi [128].
- Singular enrichment functions for elasto-plastic fracture mechanics are found in Elguedj *et al.* [71]. The proposed six-function enrichment basis is similar to the one used in [147] in meshfree methods.
- A crack tip enrichment where the sign function (19) is multiplied by a smooth function which is zero at the crack tip is proposed in Dolbow *et al.* [57]. An advantage of the resulting enrichment is that the local coordinate system (r, θ) does not need to be determined and updated during the simulation.
- Special enrichment functions for the rotation and transverse displacements near crack tips in Mindlin-Reissner plates are given by Dolbow *et al.* [58].
- Enrichment functions for arbitrary wedge shape corners in terms of eigenvalues are proposed in Duarte *et al.* [62]and applied to the edges of a solid.

5.2.3. Enrichment functions for cohesive cracks In cohesive crack models for quasi-brittle and ductile materials, the stresses and strains are no longer singular at the crack tips. Cohesive crack models suitable for metals that account for the presence of a plastic zone are proposed e.g. in [70, 18], for cementitious materials with a fracture process zone the model of [98] is widely used. In a cohesive crack, the propagation is governed by a traction-displacement relation across the crack faces near the tip. In this section only those enrichment functions which correspond to a zero-thickness cohesive process zone are considered, as e.g. in [116, 122, 124, 196].

Because the neartip fields are no longer singular for cohesive cracks, the step enrichment (21) can be suitable for the entire crack, i.e. also at the crack tip. It is, however, noted that if step enrichment is applied at all nodes in $I^\star_{\phi,\gamma}$ from (28) (with $I^\star_{\text{tip}} = \emptyset$) and is the only enrichment, the XFEM approximation is not able to treat crack tips or fronts that lie inside elements. The crack can be virtually extended to the next element edge; this approach is used by Wells and Sluys [196]. The approaches given in Duarte *et al.* [202] and Zi and Belytschko [202] overcome this deficiency and provide a method for crack tips within elements without use of singular elements.

Some references suggest special crack tip enrichments for cohesive cracks. Moës and Belytschko [124] suggest the following cracktip enrichment function

$$\psi_{\text{tip}} = r^k \sin\frac{\theta}{2}, \tag{33}$$

with k being either 1, 1.5, or 2. Other enrichment functions based on analytical considerations are given by Cox [54]. Mariani and Perego [116] developed enrichment functions consisting

of the product of the step function and polynomial ramp functions. Meschke and Dumstorff [122] use similar enrichment functions as given in (30) but with r instead of $\sqrt{r}$. Recent works on the XFEM for cohesive cracks are e.g. found by Comi and Mariani [53], Xiao *et al.* [201], Unger *et al.* [186], and Asferg *et al.* [10].

Remmers *et al.* [148] have proposed an innovative method for cohesive cracks where the discontinuity is inserted element-wise. This eliminates the need for a crack surface definition: the topology of the cracks emerges naturally as elements meet the insertion criterion and a discontinuity is injected. Motivated by this work, Song and Belytschko [164] have developed a method where cohesive segments are injected node-wise called the cracking node method.

5.2.4. Enrichments functions for dislocations The XFEM has also proved useful in continuum models of dislocations. As in cracks, dislocation solutions are characterized by discontinuities and singular points. The first application by Ventura *et al.* [191] was basically a partition of unity approach, where the regular finite element solution was enriched by the exact solution for an edge dislocation. A zone of uniformly enriched elements (flat-top) was used as in other works mentioned herein. An exact solution was adopted for the enrichment, which led to high computational expense.

Gracie *et al.* [89] explore a method where the dislocation is modeled with only a step enrichment. The approximation takes the form

$$\boldsymbol{u}^h(\boldsymbol{x}) = \sum_{i\in I} \boldsymbol{N}_i(\boldsymbol{x})\,\boldsymbol{u}_i + \boldsymbol{b}\cdot \sum_{i\in I^\star_{\phi,\gamma}} \boldsymbol{N}^\star_i(\boldsymbol{x})\cdot \psi_{\text{step,mod}}(\boldsymbol{x}), \tag{34}$$

where $\boldsymbol{b}$ is the Burgers vector, which is considered to be known. For an edge dislocation, this enrichment only introduces a jump tangent to the glide plane, thus, Eq. (34) is closely related to (16). Note that since the Burgers vector of a dislocation is known, no enrichment unknowns are introduced. The step function enrichment has to be modified (for example, by tangential regularization) at the core of the dislocation, since otherwise the field is incompatible.

In Gracie *et al.* [88] and Ventura *et al.* [190], a singular enrichment based on closed-form solutions for an edge dislocation was used around the core. The remainder of the edge dislocation was modeled by a step function enrichment. The corresponding nodal sets for the enrichments are identical to the ones given in section 5.2.2. It is noted that closed-form solutions are only readily available for isotropic materials, and in many cases anisotropic materials are of more interest in dislocation studies. XFEM models coupled to atomistic models are described in Gracie *et al.* [87]. The potential of these methods is that they circumvent the need for closed form solutions and can rely on more accurate atomistic solutions for the core. Further references on XFEM for dislocations are found in Belytschko and Gracie [25] and Oswald *et al.* [139].

5.2.5. Enrichments functions for shear bands with zero-width For shear bands, the exact structure of displacement normal to the plane of the shear band is often irrelevant to the overall response of a structure. Then, the tangential enrichment given in (16) can then be employed with the step enrichment (21) to model the shear band, see Samiego and Belytschko [155] and Réthoré *et al.* [151]. The tip of the shear band can be treated by the approach given in [202]. A method for partially accounting for the behavior through the width of the shear band is considered in Areias and Belytschko [7, 8], which is discussed in the next subsection.

5.3. High gradients

In some applications, the model of an ideal discontinuity where a property changes its value within an infinitesmal length scale is no longer justified. Instead, the structure and length scale of the variation normal to the interface is part of the solution. Examples are localization, damage, shear bands, and high gradients in convection-dominated problems. In these cases, the step enrichment may not be suitable and *regularized* step functions or subscale models are often useful. Then, the enrichment functions vary from -1 to $+1$ within a certain width across the interface.

5.3.1. Enriched nodes As long as the width of the enrichment functions is completely within the elements cut by the interface, the set of enriched nodes may be chosen as discussed in section 5.1.1 and 5.2.1 for closed and open interfaces, respectively. However, if the enrichment functions vary from -1 to $+1$ within several elements in the vicinity of the interface, it is useful to add all nodes within a certain distance from the interface for the enrichment. This is easily achieved if the interface is defined by a signed-distance function $\phi(\boldsymbol{x})$, for then,

$$I_D^\star = \{i : |\phi(\boldsymbol{x}_i)| \leq D\} \bigcup I_\phi^\star, \tag{35}$$

with $I_\phi^\star$ from (18) and D is the distance from the interface.

5.3.2. Enrichment functions We give some examples of regularized step functions. In order to be applicable in any dimension d, we express these functions in terms of the signed-distance function $\phi(\boldsymbol{x})$. The following two functions

$$\psi_{\tanh}(\phi) = \tanh(q \cdot \phi) \tag{36}$$

$$\psi_{\exp}(\phi) = \operatorname{sign}(\phi) \cdot (1 - \exp(-q \cdot |\phi|)) \tag{37}$$

are motivated from Areias and Belytschko [7] and Benvenuti *et al.* [33, 32], respectively. The parameter $q \in \mathbb{R}$ scales the gradient, for $q \to \infty$ the sign-function (19) is recovered. It is noted that these functions are only bounded by ± 1 so that there is only an indirect control over the width of the jump through the parameter q, see Fig. 13(a). A function which provides direct control over the width by the characteristic length scale $\varepsilon \in \mathbb{R}$ is

$$\psi_f(\phi) = \begin{cases} -1 & , \phi \leq -\varepsilon \\ f(\phi) & , -\varepsilon < \phi < \varepsilon \\ +1 & , \phi \geq \varepsilon \end{cases} \tag{38}$$

The function $f(\phi)$ may for example be chosen as follows [33, 142]

$$f_1 = \frac{3}{8}\tilde{\phi}^5 - \frac{5}{4}\tilde{\phi}^3 + \frac{15}{8}\tilde{\phi}, \tag{39}$$

$$f_2 = \frac{35}{128}\tilde{\phi}^9 - \frac{45}{32}\tilde{\phi}^7 + \frac{189}{64}\tilde{\phi}^5 - \frac{105}{32}\tilde{\phi}^3 + \frac{315}{128}\tilde{\phi}, \tag{40}$$

with $\tilde{\phi} = \phi/\varepsilon$, see Fig. 13(b). The function (39) is C_2-continuous at $|\phi| = \varepsilon$, whereas (40) is C_4-continuous there. The functions (36) and (37) may be used in (38) scaled form as $f = \psi_{\tanh}(\phi)/\psi_{\tanh}(\varepsilon)$ and $f = \psi_{\exp}(\phi)/\psi_{\exp}(\varepsilon)$, respectively. In these cases, there are two free parameters, q and ε, so different gradients may be present for the same width. This definition leads to C_0-continuous functions at $|\phi| = \varepsilon$.

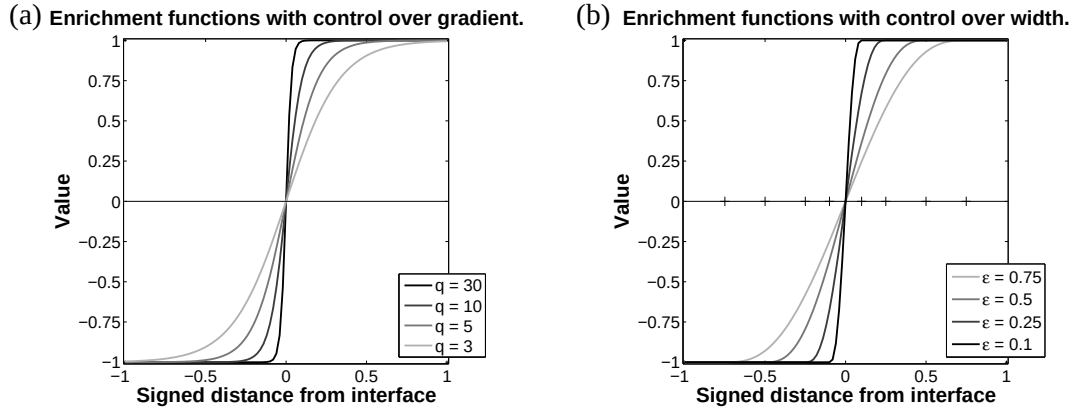

Figure 13. (a) Enrichment function (36) for different parameters q, (b) Enrichment function (39) for different parameters ε.

In some applications, the characteristic width over which the "jump" takes place may be known or estimated *a priori* and only *one* regularized step function is used for the enrichment, see Areias and Belytschko [7] and Benvenuti *et al.* [33]. In contrast, if determining the width is part of the solution *several* regularized step functions may be used with the aim to span the whole range of gradients between smooth and strongly discontinuous fields, see Patzák and Jirásek [142] and Abbas and Fries [1].

5.3.3. Applications Examples where the XFEM is used with regularized step functions are found in localization and damage where the width of the cohesive process zone is considered, see Patzák and Jirásek [142] and Benvenuti *et al.* [33, 32]. Shear bands with a characteristic length scale where the tangential displacement along the shear band localizes are investigated by Areias and Belytschko [7, 8]. Enrichments for general high gradients in convection-dominated problems are discussed in Abbas and Fries [1]; the resulting method provides highly accurate and non-oscillatory results without stabilization or mesh-refinement near shocks and boundary layers. Smith *et al.* [163] use an exponential enrichment for boundary layers in the simulation of biofilm growth.

5.4. Other enrichments and applications

Other examples for enrichment functions are briefly described below:

- Polynomial enrichments are used in the framework of the PUM in Babuška and Melenk [16, 117] and in the *hp*-cloud method by Duarte and Oden [66, 64, 136]. The aim is then an overall improvement of the solution in the sense of p-refinement in the classical FEM.
- The Laplacian is solved by GFEM on domains with inclusions or voids by Strouboulis *et al.* [171]. Later, the approach is extended to a large number of voids and also shifts in [174]. In these references, characteristic enrichment functions are computed *numerically* ("handbook" functions) before the simulation starts. Numerical handbook functions are also discussed in [172].

- Enrichment functions for the Helmholtz equation are given by Babuška *et al.* [15] and Strouboulis *et al.* [170, 173]. It is noted that the solution is oscillatory in the whole domain and, therefore, the enrichment is global.
- Enrichments for singularities in the solution of the Laplace equation near re-entrant corners are considered by Strouboulis *et al.* [169].

6. Integration

A consequence of extending the approximation space by enrichment functions $\psi(\boldsymbol{x})$ with special properties (jumps, kinks, high gradients) is that these properties are inherited by the resulting shape functions of the enrichment part, $N_i^\star(\boldsymbol{x}) \cdot \psi(\boldsymbol{x})$. This has important consequences in the quadrature of the weak form. Following the structure from section 5, we separate situations where the local enrichment functions involve a (i) discontinuity, (ii) singularity, or (iii) high gradient inside elements.

6.1. Integration for discontinuous enrichments

Consider the situation where the local enrichment functions have jumps or kinks within elements. Standard Gauss quadrature in the weak form as frequently used in the classical FEM requires smoothness of the integrands. In the presence of jumps or kinks the accuracy of Gauss quadrature and other methods that assume smoothness is drastically decreased. Therefore, for discontinuous enrichments, special procedures are required for the quadrature of the weak form.

Remark. Iarve [100] developed special regularized step functions for the enrichment for the purpose of avoiding the subdivision of elements in the quadrature of the weak form. With these regularized approximations to discontinuities, standard Gauss quadrature can be used.

6.1.1. Decomposition of elements For integration purposes, a decomposition of the elements into subelements that align with the discontinuity is standard in the XFEM. This has already been proposed in the early works on the XFEM, e.g. in [126, 29, 180]. The subelements do not have to be conforming and no new unknowns are created from this decomposition.

Let us assume that the interface is described implicitly by a discretized level-set function which is interpolated by classical FE shape functions, see equation (3), so that the zero level is given by

$$\phi^h(\boldsymbol{x}) = \sum_{i \in I} N_i(\boldsymbol{x})\, \phi_i = 0. \tag{41}$$

For simplicity, we exclude the situation where the level-set function is zero at a node, i.e. $\phi_i \neq 0$ for all $i \in I$. The interface—being the zero-level of ϕ^h—is, in general, *curved* and results from finding the roots in the *reference* element and projecting these points into the *real* element geometry (e.g. by an isoparametric mapping), see Fig. 14(a). The interface is planar inside the elements only for linear interpolants (i.e. those associated with 3-node triangular and 4-node tetrahedral elements), see Fig. 14(b). Planar interfaces enable a decomposition of the element into polygons in two dimensions and polyhedra in three dimensions.

Decomposition in two dimensions. We first consider the decomposition with respect to planar interfaces in two dimensions. Special integration formulas are available for polygons

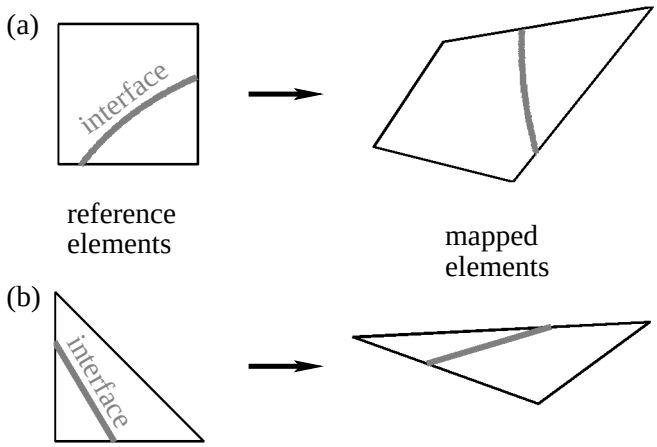

Figure 14. (a) The zero-level of $\phi^h(\boldsymbol{x})$ in a (a) bi-linear element and (b) linear element. On the left, the situation is shown in the reference element, and on the right in the real element geometry. In general, the interface is only planar for linear elements.

with n edges e.g. in Natarajan *et al.* [132]. However, often a further decomposition into quadrilaterals and triangles is useful. Then, Gauss quadrature can be employed which enables the exact integration of polynomials up to a certain order in the reference element. This property, however, is only maintained for *cut* reference elements if they are decomposed into triangular subelements, see Fig. 15(a)-(c). Using quadrilateral subelements such as in Fig. 15(d) requires an isoparametric mapping of the Gauss points into the subelements, and, although very good results may be obtained, the "exact integration" property for the reference element is lost.

For quadrilateral elements, it can be justified to replace the curved interface by a straight line, which is determined from the intersections of the interface with the element edges, see Fig. 16(b). The problem is that in this case it is difficult to construct the exact interpolation functions of $\phi^h(\boldsymbol{x})$ because they embody a constraint. Therefore, it is often preferable to decompose cut quadrilateral reference elements into triangles and use *linear* interpolation in each triangle [76, 77], see Fig. 16(c). The interface is then always piecewise straight and polygonal subelements for integration purposes are easily obtained.

Decomposition in three dimensions. In general, the interfaces described by (41) are planar only in linear tetrahedral elements. Cut tetrahedra are either a tetrahedron and a pentahedron, see Fig. 17(a), or two pentahedra, see Fig. 17(b). For hexahedral elements, where the interface is generally curved if the standard FE interpolation functions were used for $\phi^h(\boldsymbol{x})$, a decomposition into tetrahedra is useful, see Fig. 18(a). Linear interpolation is then employed within the tetrahedra and a piecewise planar interface results as shown in Fig. 18(b). It is noted that the decomposition into tetrahedra is not unique: five tetrahedra as shown in Fig. 18(a) result in opposite orientation of the diagonals at the element faces, whereas six tetrahedra can be used with identical orientation on each of two opposite faces [30]. It is noted that the assumption of a planar interface, such as shown in Fig. 16(b) for quadrilateral elements, is not applicable to hexahedral elements: Even if the interface is a straight line on the element faces of the hexahedron, the interface does not necessarily have to be a plane.

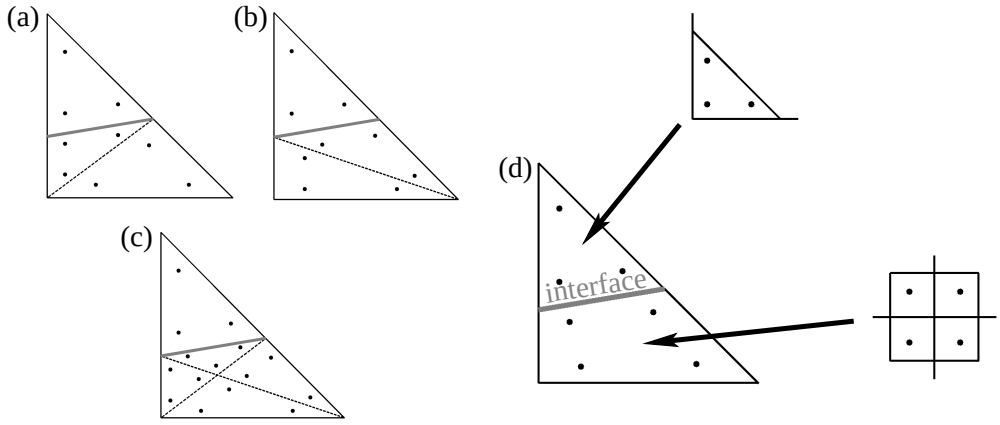

Figure 15. The interface cuts a linear reference element into a triangular and quadrilateral subelement. The quadrilateral may further be divided into triangles, (a) to (c), or not (d). Due to the bi-linear mapping, the integration points in (d) do not have the "exact integration" property which usually holds in the reference elements. It is obvious from (a) to (c) that the triangulation of the quadrilateral is not unique. Only alternative (c) is independent of the choice of a particular diagonal but more triangular subelements result.

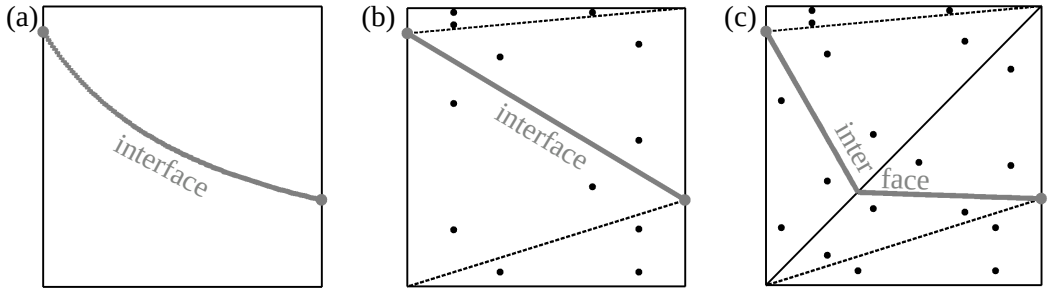

Figure 16. In general, the interface in a bi-linear reference element is curved, see (a). In order to achieve polygons for the decomposition, one may (b) either neglect the curvature by assuming a straight line between the intersections with the element edges or (c) decompose the element into two triangles and assume linear interpolation.

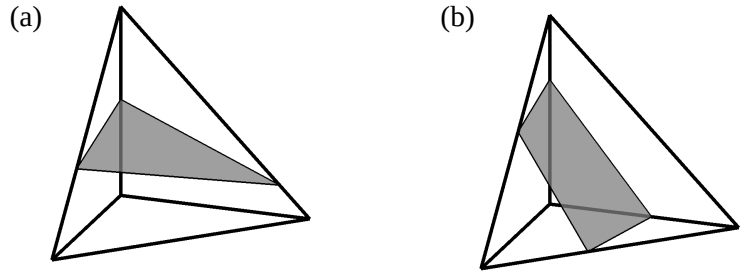

Figure 17. An interface in a linear tetrahedral elements cuts the element into (a) a tetrahedron and a pentahedron, or (b) into two pentahedra.

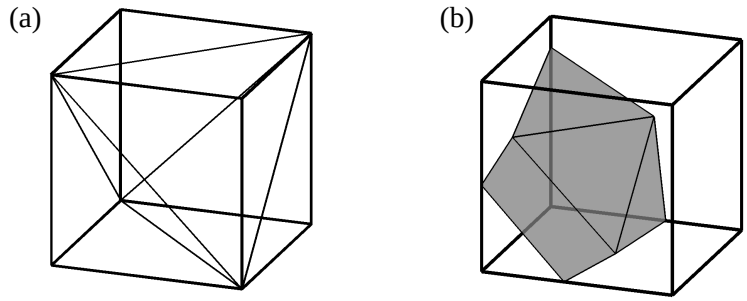

Figure 18. (a) Decomposition of a hexahedral element into five tetrahedra, (b) the interface is then piecewise planar and the decomposition into polyhedra is possible.

Decomposition for curved interfaces. A consequence of having a piecewise planar approximation of the interface is that the accuracy is somewhat limited. In higher-order applications of the XFEM, to be further discussed in section 7, it can be important to also have a higher-order description of the interface and curved interfaces can no longer be avoided. The decomposition for curved interfaces in higher-order elements is discussed in Legay *et al.* [113] and Cheng and Fries [45]. The approaches are based on an isoparametric mapping of Gauss points in a higher-order reference element into the subelements.

Explicit interfaces. It has been mentioned in section 3, that interfaces in the XFEM are often described implicitly (by the level-set method). However, especially some of the early publications use explicit descriptions by polygons, see e.g. Moës *et al.* [126] and Daux *et al.* [55] in two dimensions and Sukumar *et al.* [180] in three dimensions. For explicit descriptions, the interface is given in the real element geometry. The decomposition into subelements is then realized in the real element geometry and all integration points must be projected *backwards* into the reference element, see Fig. 19. For general elements, this requires the solution of non-linear equations for each integration point. As long as the projection is linear (general linear elements or quadrilateral/hexagonal elements whose opposite edges/faces are parallel) the extra cost is low. For more general cases, the non-linear projection can become time-consuming.

It is noted that the assumption of piecewise planar interfaces in the physical domain (i.e. in the real rather than reference element geometry) is somehow natural for crack propagation: Models typically determine planar increments during the propagation of the crack and these increments are given in the physical domain.

6.1.2. Integration by equivalent polynomials An alternative approach for the quadrature of integrands with jumps or kinks inside elements is given by Iarve [100] and by Ventura [188] and does not require the decomposition of elements. We describe the latter in more detail. Suppose that the integrand consists of an arbitrary polynomial $\mathcal{P}$ multiplied by a (strongly or weakly) discontinuous function $\mathcal{D}$,

$$\int_{\Omega_e} \mathcal{P} \cdot \mathcal{D} \, \mathrm{d}\Omega. \tag{42}$$

where Ω_e is the element domain. Then, the idea is to replace the discontinuous function $\mathcal{D}$ by a polynomial $\tilde{\mathcal{D}}$ such that the result is *exactly* the same as that obtained by the

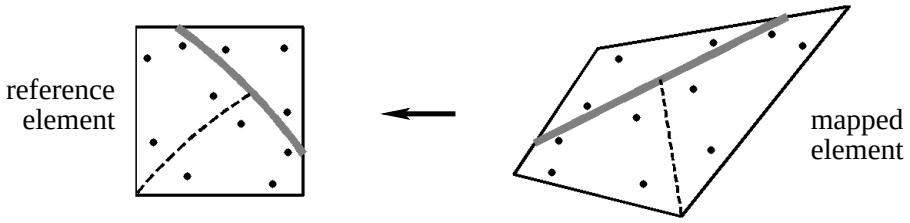

Figure 19. The decomposition for an explicit interface description is done in the real element geometry. For the evaluation of shape functions, these integration points are projected backwards into the reference element.

decomposition approach described above. The function $\tilde{\mathcal{D}}$ is called "equivalent polynomial". The order of the integrand is increased, however, the important advantage is that standard Gauss quadrature over the entire element can be employed. A drawback of this approach is that the resulting definitions of the equivalent polynomials depend on the enrichment and element type. Furthermore, for a given weak form, there may be different polynomials $\mathcal{P}$ that are multiplied by the discontinuous term $\mathcal{D}$. Then, for each case an individual equivalent polynomial $\tilde{\mathcal{D}}$ needs to be determined.

In [188], equivalent polynomials are defined for linear and bi-linear elements with enrichments for strong and weak discontinuities for linear elasticity.

6.2. Integration for singular enrichments

Special quadrature rules are also recommended for enrichment functions that are singular within elements. We do not consider the situation where the singularity coincides with an element node because this has also been studied within the classical FEM framework, see e.g. [21]. We also note that the integration of singular integrands is standard in the boundary element method [82, 183].

6.2.1. Mapping of integration points Due to high gradients near the singularity, a concentration of integration points in the vicinity of the singularity improves the results significantly. This can be achieved by using polar integration approaches as described in Laborde *et al.* [108] and Béchet *et al.* [22] for two dimensions. Laborde *et al.* [108]have shown that this approach eliminates the singular term from the quadrature. The idea is to decompose the element containing the crack tip into triangles, so that each triangle has one node at the singularity ("singularity node"). Tensor-product type Gauss points in a quadrilateral reference element are mapped into each triangle such that two nodes of the quadrilateral coincide at the singularity node of each triangle. The procedure is depicted in Fig. 20. This approach is well-suited for point singularities; however, the extension to three dimensions where a singularity may be present along a front may be difficult as noted in [108, 22].

The idea of using special mappings is further extended by Park *et al.* [141] which is also applicable to three dimensions. Special integration points and weights are used which capture the singularity either at a node or along an edge (of a subelement resulting from a decomposition).

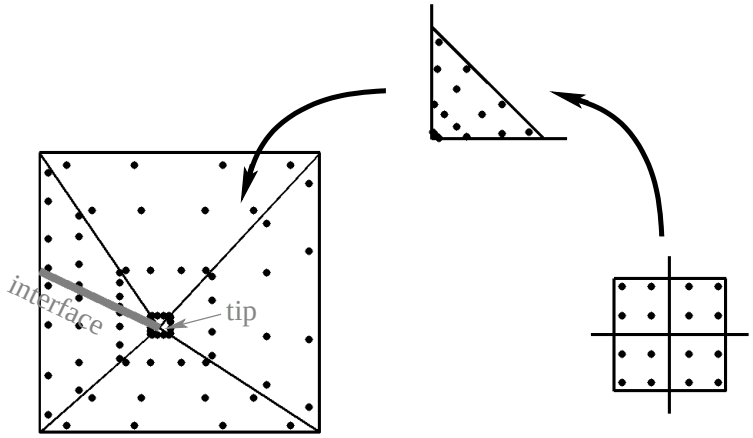

Figure 20. Integration points in an element containing a singularity. Standard Gauss points are projected from a quadrilateral element into a triangular element. The triangular element is then projected into the element containing the singularity such that the integration points are concentrated at the singularity.

6.2.2. Integration along contour integrals A transformation of the integration domain containing the singularity into a contour integral is proposed by Ventura *et al.* [190] for crack and dislocation enrichments in the framework of linear elasticity. Contour integrals are evaluated with much less computational effort than domain integrals. These methods can also be used to reduce domain integrals to surface integrals in three dimensional problems. The method is only applicable to elements for which all nodes of the element are enriched and for which all enriched degrees of freedom at all nodes of the element are equal [190], i.e. for flat-top enrichments. Furthermore, the enrichments must be (nearly) equilibrium solutions of the underlying problem.

6.2.3. Adaptive integration Adaptive integration for elements with singularities is used e.g. in Strouboulis *et al.* [169, 171], Liu *et al.* [115], and Xiao and Karihaloo [200]. However, as noted in [200], an adaptive control of the integration error can be very time-consuming.

6.3. Integration for high gradient enrichments

For high-gradient enrichments such as those with regularized step functions, the integrand may be continuous, however, a large number of Gauss points may be needed in order to yield accurate results. This approach has for example been used by Abbas and Fries [1] for simplicity. It is often useful to concentrate integration points where they are needed i.e. in the narrow region around the maximum gradient as e.g. realized by Areias and Belytschko [7]. In Benvenuti *et al.* [33], adaptive integration is used and a new technique is introduced which is based on the equivalent polynomial approach of section 6.1.2. These approaches are compared with standard Gauss integration showing the large benefit of the advanced integration methods.

6.4. Integration along interfaces

It is sometimes necessary to evaluate terms in the model equations along the interface. For example, in Dolbow *et al.* [59], the integration on a crack surface with contact is discussed. The interface is piecewise linear. Another example are two-phase flows with surface-tension, which has been realized for quadrilateral elements in two dimensions in Fries [77]. Then, the interface in the real element geometry is not necessarily piecewise linear which renders the evaluation of geometric quantities (normal vector, curvature) more complicated. For three-dimensional applications, computing the positions and weights of integration points on the interface is a mathematically simple yet computationally demanding task.

7. Higher-order XFEM

Two different strategies for achieving higher-order results with the XFEM/GFEM are distinguished. For simplicity, we focus on the inclusion of *one* special solution property into the approximation space through the enrichment function $\psi(\boldsymbol{x})$.

7.1. p-XFEM through polynomial enrichments

One strategy is to use low-order partition of unities $\{N_i^\star(\boldsymbol{x})\}$ and to "improve" the enrichment by a multiplication of $\psi(\boldsymbol{x})$ with a basis vector $\boldsymbol{p}(\boldsymbol{x})$ which consists of monomials up to a certain order. Then, several enrichments based on $\psi(\boldsymbol{x})$ result as

$$\boldsymbol{\psi}(\boldsymbol{x}) = \psi(\boldsymbol{x}) \cdot \boldsymbol{p}(\boldsymbol{x}) . \tag{43}$$

An example for the basis vector is $\boldsymbol{p}^{\mathrm{T}} = [1, x, y, x \cdot y]$ in two dimensions. Often, Legendre polynomials are used. This approach with $\psi(\boldsymbol{x}) = 1$ has been intensively investigated in the frame of the PUM [117, 16], GFEM [169, 20, 19] and *hp*-cloud method [66, 62, 136]. As $\psi = 1$ is used, the aim is not to introduce a special solution property in the sense of section 2 but to improve the overall accuracy closely related to *p*-adaptivity in the classical FEM. This can be interpreted as a "polynomial enrichment". Realizations where the step enrichment ψ_{step}, see section 21, is used in (43) are discussed in Mariani and Perego [116], Duarte *et al.* [65] and Perego *et al.* [144]. The abs-enrichment ψ_{abs} for weak discontinuities, see section 23, is multiplied by $\boldsymbol{p}(\boldsymbol{x})$ in Cheng and Fries [45]. A consequence of using the improved enrichment functions (43) is that at each node (of the low-order elements) several unknowns resulting from the enrichment are present. Linear dependencies of the basis are a major issue in this approach.

7.2. p-XFEM through higher-order elements

The second strategy only makes use of the enrichment function $\psi(\boldsymbol{x})$, which is chosen as described in section 5. Higher-order accuracy is then achieved by using classical higher-order FE shape functions for $N_i(\boldsymbol{x})$ (and often $N_i^\star(\boldsymbol{x})$) in the extended approximations given in section 4. For example, the shape functions of hierarchical FEs [126], spectral FEs [113], or higher-order Lagrange elements [175, 45] have been applied.

In what follows, we focus on higher-order applications for *discontinuities*. There the majority of the publications follow the second strategy described above. It is important to note that the

description of the interface is formally independent of the approximation. That is, in higher-order applications of the XFEM, the interface may still be considered (piecewise) planar. Most publications assume planar interfaces in order to facilitate the quadrature, see section 6. However, it can be expected that if the physical problem involves curved interfaces, both a higher-order description of the approximation *and* the interface is required for optimal convergence rates; this is confirmed e.g. by Cheng and Fries [45]. Furthermore, for higher-order accuracy, it is crucial to circumvent the pathologies in blending elements such as discussed in section 4.3.

Remark. We note that there are other motivations for using higher-order elements besides achieving higher-order accuracy: In Chessa *et al.* [51], hierarchical shape functions are used locally to improve the performance of the blending elements. In Mariani and Perego [116], higher-order functions are used in order to reproduce the typical cusp-like shape of the process zone at the tip of a cohesive crack. In Iarve [100], higher-order functions are used to replace the step function and enable standard Gauss quadrature in the cut elements.

7.2.1. Straight discontinuities. We first consider higher-order XFEM approximations for (piecewise) planar interfaces. The use of higher-order hierarchical elements has already been proposed by Moës *et al.* [126]. In Wells and Sluys [196] and Wells *et al.* [197], 6-node triangles are used for the approximation. However, in the previous references, no convergence results are discussed. Careful convergence studies with higher-order accuracy for planar cracks are realized by Laborde *et al.* [108] and Tarancón *et al.* [185]. There, in agreement with the findings for linear elements by Béchet *et al.* [22] and later Fries [78], it is shown that in order to obtain optimal accuracy for the singular problem of elastic fracture mechanics, (i) the crack tip enrichment should be applied in a fixed area around the crack tip as the mesh is refined (section 5.2.1), (ii) advanced integration techniques for the element containing the crack tip are required (section 6.2.1), and (iii) blending elements must be treated appropriately (section 4.3). In the study of higher order elements in [108], blending elements are avoided by coupling fully enriched and standard elements point-wise, while in [185], hierarchical shape functions are used in the blending elements.

7.2.2. Curved discontinuities. Higher-order descriptions of the interface in the frame of the XFEM have been considered e.g. by Stazi *et al.* [165] and Zi and Belytschko [202]. In these papers, for integration purposes, the interface is still assumed to be straight and a decomposition into subelements is realized as described in section 6.1.1. In the results obtained by [165], the absolute value of the error is improved compared to the linear case, but the rate of convergence is not improved. In Legay *et al.* [113], spectral elements are used for curved strong and weak discontinuities; the curvature is accounted for in the quadrature. Problems in blending elements are reduced by using shape functions $N_i^\star$ of at least one order lower than the shape functions N_i of the standard FE part. However, optimal convergence is achieved only for *straight* discontinuities; for curved discontinuities the results are improved, but not quite optimal. Optimal rates of convergence for curved strong and weak discontinuities have recently been obtained by Cheng and Fries [45]. The higher-order shape functions are based on Lagrange elements and a special integration technique is proposed. Problems in blending elements are avoided by using the corrected XFEM, see section 4.3, which enables the use of the same order for N_i and $N_i^\star$.

8. Time-integration in the XFEM

Let us assume that the governing equations under consideration are time-dependent on a fixed domain Ω. As long as the enrichment functions $\psi(\boldsymbol{x})$ in the extended approximations of section 4 are *independent* of the time, time integration methods used in the classical FEM may be used for the XFEM and will exhibit similar accuracy.

However, in most transient problems, the location of a discontinuity or high gradient moves in time. Examples are dynamic crack propagation, moving interfaces between two fluids etc. As discussed in section 3, the level-set method may as well be applied for the description of moving interfaces, leading to a time-dependent level-set function $\phi(\boldsymbol{x}, t)$. Consequently, enrichment functions that involve the level-set function are also time-dependent, i.e. $\psi(\boldsymbol{x}, t)$. The important difference compared to classical FE approximations on fixed meshes is that the basis functions in *extended* approximations are usually not constant in time. This may have serious implications for the time-integration schemes employed in XFEM [48, 49, 81].

Remark. It is noted, that the presence of a model for the underlying physics and for the interface movement leads to a *coupled problem* in the sense of Felippa and Park [73]. Typically, partitioned schemes are employed for the solution. It depends on the application whether the interaction between the fields should be considered in a strongly or weakly coupled scheme. For strong coupling, several iterations are needed within one time-step.

8.1. Time-stepping

In Fries and Zilian [81], several one-step time-stepping schemes are analyzed for moving weak discontinuities. In order to point out some important properties about the XFEM in time-stepping schemes it is useful to consider the following one-dimensional model problem: A domain Ω with boundary $\Gamma = \partial\Omega$ is divided into two time-dependent subdomains $\Omega_1 = (0, x^\star(t))$ and $\Omega_2 = (x^\star(t), 1)$. The initial/boundary value problem consists of finding $u(x,t)$ for all $x \in \Omega$ and $t \in (0,T)$ such that

$$u_{,t} = k_i \cdot u_{,xx} \qquad \text{in } \Omega_i \times (0,T),\ i = 1,2, \tag{44}$$

$$u(x,t) = \hat{u}(x,t) \qquad \text{on } \Gamma \times (0,T), \tag{45}$$

$$k_1/k_2 \cdot u_{,x}(x^\star - \varepsilon, t) = u_{,x}(x^\star + \varepsilon, t) \text{ for } \varepsilon \to 0, \tag{46}$$

$$u(x,0) = u_0(x) \qquad \text{on } \Omega \text{ at } t = 0. \tag{47}$$

The diffusion coefficients $k_1, k_2 \in \mathbb{R}$, $k_1 \neq k_2$, are discontinuous at a moving point $x^\star(t) \in \Omega$. As a result the scalar function $u(x,t)$ has a weak discontinuity at $x^\star$. The trapezoidal rule is used in time with time-step size Δt; t_n and t_{n+1} refer to the previous and current time step, respectively. Then, the discretized weak form is: Given u_0^h, find $u^h \in \mathcal{S}^h$ such that $\forall w^h \in \mathcal{V}^h$

$$\frac{1}{\Delta t}\int w^h (u_{n+1}^h - u_n^h)\mathrm{d}\Omega + \frac{1}{2}\int k_{n+1} w_{,x}^h \cdot (u_{n+1}^h)_{,x}\mathrm{d}\Omega + \frac{1}{2}\int k_n w_{,x}^h \cdot (u_n^h)_{,x}\mathrm{d}\Omega = 0, \tag{48}$$

where $\mathcal{S}^h$ and $\mathcal{V}^h$ are suitable test and trial function spaces spanned by the classical FE shape functions *and* the enrichment functions. Furthermore, as shown in Fig. 21(a) and (b),

$$u_m^h = u^h(x, t_m) = \sum_{i \in I} N_i(x)\, u_i + \sum_{i \in I^\star} N_i^\star(x) \cdot \psi(x, t_m)\, a_i \tag{49}$$

and

$$k_m = k(x, t_m) = \begin{cases} k_1 & \text{for } x \leq x^\star(t_m), \\ k_2 & \text{else.} \end{cases} \tag{50}$$

The following findings hold for (48): (i) As noted by Chessa and Belytschko [48], there is an ambiguity in the choice of the test function w^h, i.e. in the time selected for the test functions; the admissible test functions vary with time so more than one choice can be made. It is shown by Fries and Zilian [81], that $w^h = w^h_{n+1}$ is required in order to ensure the regularity of the system matrix. (ii) In each time step, in order to evaluate u^h_{n+1} and u^h_n correctly, the enrichment functions $N^\star_i(x) \cdot \psi(x, t_m)$ must be evaluated at t_n *and* t_{n+1}. (iii) For an appropriate quadrature of those parts in the weak form (48) which include terms corresponding to time-level t_n and t_{n+1}, the elements have to be decomposed into subelements with respect to the interfaces defined by $\phi(x, t_n)$ *and* $\phi(x, t_{n+1})$, see Fig. 21(c). It is thus seen that time-stepping in the XFEM requires special care if convergence rates higher than 1 in the L_2-norm are to be achieved.

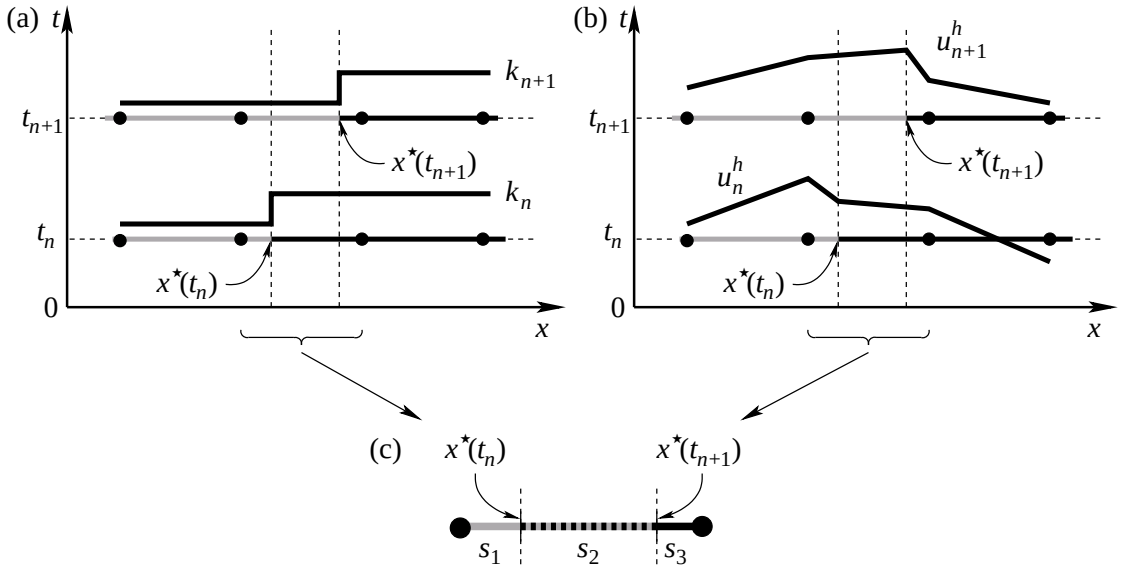

Figure 21. (a) and (b) show examples for k_m and u^h_m with $m = n, n+1$. (c) The presence of inner-element discontinuities defined by $\phi(x, t_n)$ and $\phi(x, t_{n+1})$ must be considered in the quadrature for optimal accuracy.

Dynamic crack growth. Another example of moving interfaces are propagating cracks. As mentioned in section 3, in a crack growth model, while the crack front changes with time, the existing crack surface remains unchanged. Moreover this application involves time discontinuities which are not properly treated in many time-stepping schemes, as noted e.g. by Réthoré *et al.* [150]. Special tip enrichment functions such as those used for static problems (section 5.2) present difficulties in dynamics. Therefore, a modified step enrichment is proposed in [24] which allows for inner-element crack tips. The enrichment is suitable for cohesive cracks; a related method is given by Zi and Belytschko [202]. This enrichment is compatible with the original step enrichment along the crack path and allows for a smooth transition.

Implicit time-integration by Newmark-type methods is discussed by Réthoré *et al.* [150]. In Menouillard *et al.* [118], the Newmark method is used with a lumped mass matrix in order to achieve an explicit formulation. The problem of the critical time step tending to zero when the crack approaches a node is avoided by using a special lumping strategy which results in a critical time step of the same order of magnitude as the critical time step for a standard FE mesh. This approach is further investigated in Menouillard *et al.* [119].

8.2. Space-time finite elements

In Chessa and Belytschko [48], a discontinuous space-time Galerkin method is proposed for transient problems in the XFEM with first-order partial differential equations in one dimension. The method is based on a generalized space-time variational principle from which the Rankine-Hugoniot conditions emanate naturally. The dependent variable is approximated in space and time by finite elements with discontinuities in space-time, so the dimension of the finite elements is increased by one over the number of space dimensions. Space-time finite elements appear to be a natural choice for the time-dependent XFEM as the movement of the enrichment and interfaces in space-time can be treated consistently. This has also been confirmed for time-dependent problems with second-order time-derivatives (crack propagation) in Réthoré *et al.* [149].

For the model problem given above the procedure is as follows: The space-time domain $\Omega\times(0,T)$ is divided into time slabs $Q_n = \Omega\times(t_n, t_{n+1})$, where $0 = t_0 < t_1 < \ldots < t_{\mathrm{N}} = T$. Each time slab is discretized by extended space-time finite elements. The enriched approximation is of the form

$$u^h(x,t) = \sum_{i\in I} N_i(x,t)\, u_i + \sum_{i\in I^\star} N_i^\star(x,t)\cdot\psi(x,t)\, a_i \tag{51}$$

where $N_i(x,t)$ are two-dimensional finite element functions. The discretized weak form may be formulated as follows: Given $\left(u^h\right)_n^-$, find $u^h \in \mathcal{S}_n^h$ such that $\forall w^h \in \mathcal{V}_n^h$

$$\int_{Q_n} w^h \cdot u^h_{,t}\, dQ + \int_{Q_n} k(x,t)\; w^h_{,x}\cdot u^h_{,x}\, dQ \tag{52}$$

$$+ \int_{\Omega_n} \left(w^h\right)_n^+ \cdot \left(\left(u^h\right)_n^+ - \left(u^h\right)_n^-\right) d\Omega \;=\; 0, \tag{53}$$

where $\left(u^h\right)_n^\pm$ is

$$\left(u^h\right)_n^\pm = \lim_{\varepsilon\to 0} u^h(x, t_n \pm \varepsilon), \tag{54}$$

and

$$k(x,t) = \begin{cases} k_1 & \text{for } x \le x^\star(t), \\ k_2 & \text{else,} \end{cases} \tag{55}$$

see Fig. 22.

Convergence studies for linear space-time elements are presented by Fries and Zilian [81] and for higher-order space-time elements by Cheng and Fries [45]; optimal convergence rates have been achieved. However, the computational effort in space-time finite elements is significantly increased compared to customary time-stepping schemes as finite elements with one dimension higher than the spatial dimensions are used. Especially for three-dimensional problems in space, the use of four-dimensional space-time elements (which, in addition, need to be decomposed

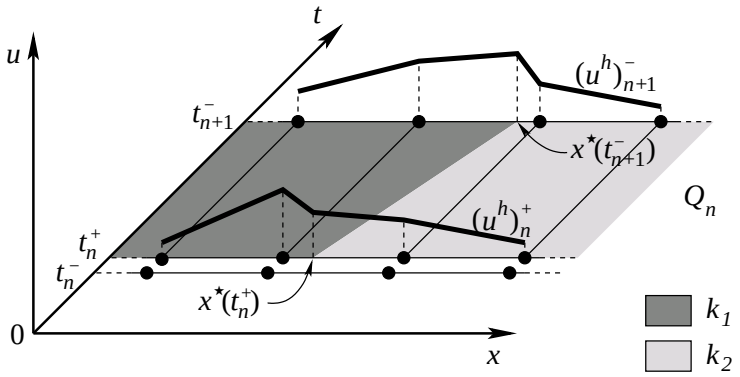

Figure 22. The approximations $\left(u^h\right)^{\pm}_m$ with $m = n, n+1$ and the parameters k_1 and k_2 in the space-time domain.

into subelements for the quadrature) has not yet been reported in XFEM applications. With the aim to decrease the computational effort of space-time elements, a hybrid approach was proposed by Chessa and Belytschko [49]. Space-time elements are only used in the elements cut by the discontinuity, otherwise standard time-stepping is used.

9. Interface and boundary conditions

For the discussion of interface and boundary conditions in the XFEM, it is useful to define an elliptic, second-order model problem following Zilian and Fries [206]. The boundary value problem is related to the Poisson equation and consists of finding $u(\boldsymbol{x})$ for all $\boldsymbol{x} \in \Omega$ such that

$$k_i \Delta u = f \quad \text{in } \Omega^i,\ i = 1, 2, \tag{56}$$

$$u = g \quad \text{on } \Gamma^i_g, \tag{57}$$

$$k_i \nabla u \cdot \boldsymbol{n}_\Gamma = h \quad \text{on } \Gamma^i_h, \tag{58}$$

$$u_i = g_\Sigma \text{ on } \Sigma_g, \tag{59}$$

$$k_i \nabla u_i \cdot \boldsymbol{n}_\Sigma = h_\Sigma \text{ on } \Sigma_h, \tag{60}$$

$$[\![u]\!] = j_\Sigma \text{ on } \Sigma_c. \tag{61}$$

The interface $\Sigma = \Sigma_g \cup \Sigma_h \cup \Sigma_c$ decomposes the domain $\Omega \in \mathbb{R}^d$ into the disjoint domains Ω^1 and Ω^2 with outer boundaries Γ^1 and Γ^2 such that $\Omega = \Omega^1 \cup \Omega^2$ and $\Gamma = \Gamma^1 \cup \Gamma^2$, see Fig. 23. The model parameters $k_i \in \mathbb{R}$ are constant in Ω^i and discontinuous at Σ, i.e. $k_1 \neq k_2$. Only in this section, we use this differing nomenclature for the outer boundary and the interface.

It is thus seen that the boundary value problem includes boundary and interface conditions. Equations (57) and (58) are Dirichlet and Neumann boundary conditions, respectively. Equations (59), (60), and (61) are constraints on the interface Σ. A Dirichlet-type constraint is given in (59) and enforces values for the primal variable u, a Neumann-type constraint is present in (60) and enforces flux values, and (61) prescribes the jump along Σ, where $[\![\cdot]\!] = (\cdot)_1 - (\cdot)_2$.

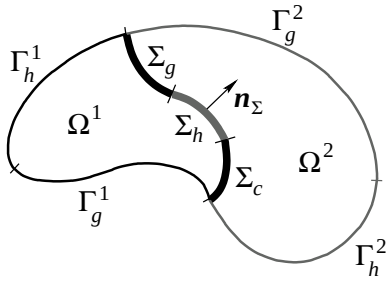

Figure 23. The domain $\Omega = \Omega^1 \cup \Omega^2$ with boundary $\Gamma = \Gamma_g^1 \cup \Gamma_h^1 \cup \Gamma_g^2 \cup \Gamma_h^2$ and interface $\Sigma = \Sigma_g \cup \Sigma_h \cup \Sigma_c$. Different types of constraints are enforced on the boundary and the interface.

9.1. Boundary conditions

We assume that the domain is discretized by a conforming mesh. Referring to the model problem given above, boundary conditions are applied along the Dirichlet boundary $\Gamma_g^1 \cup \Gamma_g^2$ and the Neumann boundary $\Gamma_h^1 \cup \Gamma_h^2$. The imposition of Neumann boundary conditions is straightforward in the XFEM and is realized as in the classical FEM (by evaluating corresponding integrals in the weak form along the Neumann boundary). However, Dirichlet conditions, see (57), may require special attention. We only consider the situation where the enrichment is present at the boundary (e.g. because the interface crosses the boundary), otherwise, also for the Dirichlet boundary conditions, the situation is the same as in the classical FEM.

For the case that the extended approximation is *not* shifted, the shape functions involved do not have the Kronecker-δ property and, as a consequence, $u^h(\boldsymbol{x}_i) \neq u_i$. The imposition of Dirichlet boundary conditions is then very similar to the situation frequently observed in meshfree approximations, see e.g. Fernández-Méndez [74] and Griebel and Schweitzer [94]. It is then useful to impose the Dirichlet conditions weakly, e.g. by Lagrange multipliers.

For the standard case of shifted approximations, the Kronecker-δ property is recovered because the enrichment functions $N_i^\star \cdot [\psi - \psi_i]$ vanish at the nodes. We note that between the nodes, the enrichment functions do not vanish in general. It is straightforward to apply *smooth* boundary conditions for applications with extended approximations: Assume that the value g_i is to be applied at the enriched node i with the degrees of freedom u_i and a_i, then we set $u_i = g_i$, $a_i = 0$. On the other hand, for non-smooth boundary conditions (i.e. those which have an inner-element jump or kink along the Dirichlet boundary), the values for the enriched degrees of freedom are usually not known. One may either find the values for a_i such that the kink/jump is accounted for correctly by solving a (local) interpolation problem prior to the calculation or impose the Dirichlet conditions weakly.

We mention that although special considerations are sometimes needed, the imposition of boundary conditions in XFEM applications is in most cases not troublesome. Therefore, this issue has received much less attention in the XFEM than for meshfree methods.

9.2. Interface conditions

Now we focus on enforcing constraints along the interface Σ inside elements. Practical applications are found for example in crack propagation with frictional contact [59, 105],

thermal and phase change problems [121, 123, 50], and fluid-structure interaction [207]. We also mention the case where the domain is immersed in a non-conforming mesh [29, 30, 123]. Then, *boundary* conditions are applied inside elements and the situation is identical to applying Dirichlet-type and Neumann-type constraints such as (59) and (60) at an inner-element interface.

In general, enforcing constraints is typically done by means of the following approaches [28]: (i) the penalty method, (ii) Lagrange multipliers, and (iii) Nitsche's method. All these approaches have been employed for enforcing interface constraints in the XFEM.

Penalty method. In this method, no additional unknowns result, but the conditioning of the system matrix scales with the order of the penalty parameter which enforces the constraint. This approach is used by Chessa *et al.* [50], Ji and Dolbow [103], and Liu and Borja [114] in the XFEM.

Lagrange multipliers. When Lagrange multipliers are used, additional unknowns are present and a mixed method is obtained. The Lagrange multiplier space must be chosen carefully so as to satisfy the "inf-sup" condition [11, 37]. The choice of the Lagrange multiplier space is not unique. A particularly simple strategy is to use multipliers based on the surface mesh that naturally arises from the intersection of the interface with the mesh in the domain, see Fig. 24. However, as shown in Ji and Dolbow [103] and Moës *et al.* [123], this "convenient" choice leads to oscillations in the multiplier and decreases the overall convergence rate. This may be traced back to an over-constrained primal variable space. Two approaches have so far been reported which are based on a convenient approach but achieve optimal results: One strategy obtains stable multipliers by either omitting certain intersections of the interface with element edges, see Moës *et al.* [123], or by placing multipliers on the interface inside elements, see Kim *et al.* [105]. The second strategy is to stabilize the convenient approach and is discussed by Mourad *et al.* [131] and Dolbow and Franca [60]. Perturbed distributed Lagrange multipliers which are placed at the nodes in the cut elements and are associated with shape functions of the same spatial dimension than Ω are used in Zilian and Legay [207] for enforcing the continuity in a step enriched setting; a stabilization parameter is needed in this approach.

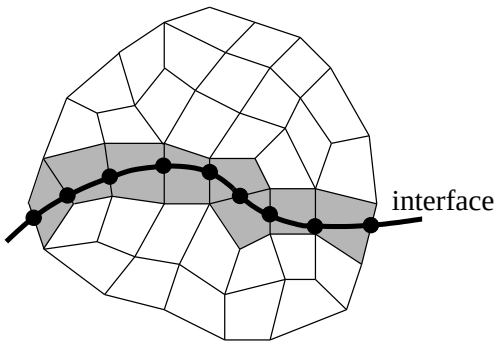

Figure 24. The most convenient choice for the Lagrange multipliers are the intersections of the interface with the element edges. One-dimensional hat functions are then employed inbetween the multipliers. However, this approach leads to sub-optimal convergence rates.

Nitsche's method. This method can be considered as a consistent penalty method. It does

not introduce additional unknowns, however, a stabilization parameter has to be specified. The conditioning of the system matrix is not largely affected. Nitsche's method is used in Hansbo and Hansbo [96] in a finite element procedure which is closely related to the XFEM as shown in [6]. A form of Nitsche's method was also developed for the Hansbo and Hansbo approach by Dolbow and Harari [56]; both discontinuities in the function and gradient were treated, with either or both as prescribed. A mathematical analysis was given for selecting effective penalty parameters.

Other approaches. In [59, 121] the LATIN method [109] is used for enforcing constraints. The key feature of the LATIN method is to separate a problem into a simple (linear), global part and a more complicated (often non-linear) local part; the coupled problem is then solved iteratively. In the applications discussed in [59, 121], the local problem is the interface constraint. Another approach for enforcing constraints in the XFEM is proposed in [120]. There, continuity across the interface is imposed weakly by means of the interior penalty method in the frame of the discontinuous Galerkin method. A new approach which is based on the reformulation of Equations (56) to (61) near the interface in terms of a mixed method is presented in Zilian and Fries [206]. This gives access to flux-values and enables the imposition of arbitrary constraints. The flux-variables are condensed statically so that the resulting global system consists of the primary variable only.

10. Error estimation and adaptivity

Error analysis is crucial in assessing the quality of a solution. Two strategies exist in error estimation: *A priori* error estimation is concerned with the derivation of bounds for the approximation error based on the properties of the approximation, and can therefore be performed prior to the calculation, whereas *a posteriori* error estimation is aimed at estimating the error of an existing numerical solution. *A posteriori* error estimation falls into two classes: residual based and recovery based estimation. The interested reader is referred to [3, 4] for a good treatment of error estimation in the framework of the classical FEM.

The early works on the PUM and GFEM provide a sound mathematical foundation of approximations that are based on the partition of unity concept. Error estimates in the PUM have been reported by Melenk and Babuška [117, 16] and in the GFEM e.g. by Strouboulis *et al.* [169, 176].

Most error estimation procedures that have so far been reported in the XFEM are realized with recovery based estimation. These methods rely on the computed stress field which results by direct differentiation of the approximation and an improved "recovered" stress field. A stress recovery by means of the moving least-squares (MLS) method is discussed by Xiao and Karihaloo [200]. This approach is based on [184] for the classical FEM. In [200], standard polynomial basis functions are employed for the MLS approximation. The use of *enriched* basis functions in the MLS approximation has been proposed by Bordas *et al.* [35, 34]. Note that the enrichment is *intrinsic* in this case as in extended meshfree methods, see Fleming *et al.* [75], or in the intrinsic XFEM by Fries and Belytschko [78]. In Duflot and Bordas [69], the global derivative recovery, as proposed in [135] for the FEM, is extended to enriched finite elements and an associated error indicator is derived. An adaptation of the superconvergent patch recovery for the XFEM framework is presented by Ródenas *et al.* [152]. This recovery technique has first been proposed for the classical FEM in [204, 205].

We do consider classical h- and p-adaptivity nor do we further elaborate on (adaptive) polynomial enrichment in the PUM/GFEM/hp-clouds which has been mentioned in section 7. Instead, we limit ourselves to cases where the enrichment functions for discontinuities and high gradients as discussed in section 5 are used in an adaptive procedure. This kind of adaptive enrichment may be labeled "e-adaptivity" as suggested in [69]. It is then clear that the polynomial enrichment mentioned before in an adaptive procedure may either be considered as a special kind of e-adaptivity with polynomials or as a non-classical type of p-adaptivity.

A set of regularized step functions, see section 5.3, was first used in an adaptive procedure by Pathák and Jirásek [142] for cohesive cracks. The computation starts with a classical FE approximation, that is, no enrichment functions are employed. The enrichment functions are activated during the simulation when needed. In Waisman and Belytschko [195], an adaptive enrichment procedure is suggested which determines characteristic parameters of the enrichment functions during the simulation. For boundary layers an enrichment function of $\psi(s) = \exp(-\alpha \cdot s)$ is suggested where s is a coordinate normal to the boundary and α is determined during the simulation. Another example are singular fields, where the enrichment function may be chosen as $\psi(r) = r^{\alpha}$ where r is the polar coordinate with the singularity at $r = 0$ and α is an adaptively chosen parameter which reflects the character of the singularity. In Duflot and Bordas [69], the optimal radius of enriched nodes around a crack tip is determined adaptively. Once this radius is specified, the authors suggest to use classical h/p-adaptivity.

11. Linear dependence and ill-conditioning

In some situations, the approximation space spanned by the functions in the extended approximations given in section 4 is (almost) linearly dependent.

For the enrichment functions proposed in the early works on the PUM [117, 16] and GFEM [169], and especially for the case of polynomial enrichments (i.e. where a low-order partition of unity is enriched by polynomials such that a higher-order approximation results) linear dependencies are a major issue. It is mentioned in [16] (p. 729) that finding a basis of the PUM space and controlling the condition number of the stiffness matrix created by the PUM is one of the key aspects which have to be addressed. Modifications of the partition of unity functions $N_i^{\star}$ are proposed in order to avoid linear dependencies. In [169], where the partition of unity is constructed by classical FE shape functions, linear dependencies are resolved on the level of the solver for the system of equations.

For extended approximations which use locally enriched nodes with the aim to capture discontinuities and/or high gradients, linear dependencies are less frequently observed and often identified easily. We find two typical situations:

1. Element matrices of cut elements whose nodes are enriched by the step function, see section 5.1.2, are ill-conditioned if the ratio of the areas/volumes on both sides of the discontinuity is very large, see Fig. 25. It is often useful to remove the enrichment of those nodes whose enrichment functions have only small supports in the cut element, see e.g. Bordas *et al.* [36], Liu *et al.* [115], and Daux *et al.* [55]. Furthermore, if the discontinuity is allowed to cut directly through a node or to align with an element edge/face, special considerations are required. However, for discontinuities which are described by the level-set method, this is easily avoided by enforcing $\phi(\boldsymbol{x}_i) \neq 0$.

2. When special enrichment functions are used at the front of an interface (e.g. crack tip enrichments), and all nodes within a prescribed, given distance from the interface front are enriched, see section 5.2, the condition number of the resulting system of equations increases markedly for h-refinement. The situation is improved by clustering the nodes of the enriched subdomain so that only one degree of freedom exists for one or more sets of these enriched nodes, i.e. the flat-top procedure, see Laborde *et al.* [108] and Ventura *et al.* [190]. An alternative is the pre-conditioning of the matrices as proposed by Béchet *et al.* [22].

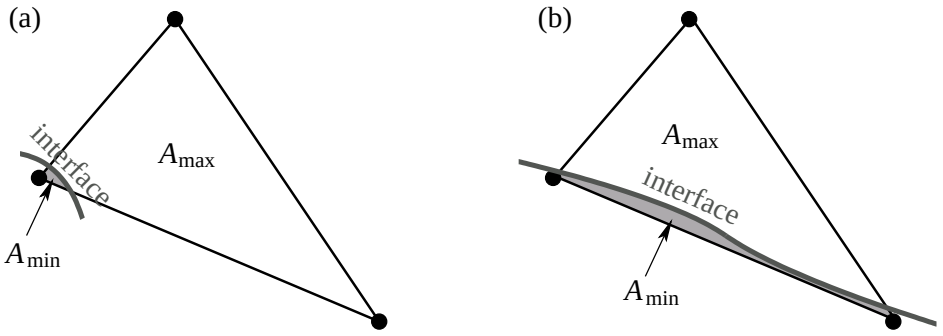

Figure 25. The interface is close to (a) a node or (b) an edge, respectively. As a result, the ratio $A_{\max}/A_{\min}$ is very large, leading to ill-conditioned matrices for step enriched elements.

12. Implementation

In an XFEM code, there are at least three major differences compared to a classical FE code: (i) The quadrature has to consider the special character of the enrichment, see section 6, (ii) the enrichment functions have to be implemented, see section 5, and (iii) the code must be able to deal with a variable number of degrees of freedom per node which holds on the element-level (the element matrices have different dimensions) as well as for the overall system matrix. Furthermore, concerning the post-processing, it is mentioned that for the visualization of results with inner-element discontinuities adjustments in the visualization tools may be advisable. It depends on the particular application if special care is needed for the time-integration (section 8), the boundary and interface conditions (section 9), and linear dependencies (section 11).

Especially the third aspect mentioned above—the variable number of degrees of freedom per node—may lead to significant problems if the XFEM is to be incorporated into an existing FE code and may require substantial background knowledge of the user. (This can be avoided by assigning the enrichment unknowns to additional nodes, e.g. a 4-node bilinear quadrilateral with a discontinuity enrichment would be implemented as an 8 node bilinear quadrilateral with the extra four nodes storing the enrichment). Variable number of degrees of freedom per node may also be awkward with respect to parallelization of the code. However, for implementations which consider the needs of the XFEM from the beginning, the computational effort scales exactly like a classical FE simulation. It is noted that, for a given level of accuracy, the XFEM

often requires far fewer degrees of freedom *and* computational effort for the problems we have described than a corresponding classical FE simulation.

References that describe the implementation of the XFEM in detail—on the level of algorithms, functions and variable names—are given by Bordas *et al.* [36], Nistor *et al.* [133], and Sukumar and Prévost [181]. The focus in these references is on modeling of cracks. The implementation of the XFEM into the commercial FE software Abaqus is discussed by Giner *et al.* [85].

13. Conclusions

We have given an overview of the extended finite element method (XFEM) and the generalized finite element method (GFEM) with an emphasis on XFEM methods for discontinuities and high gradients. The majority of this work has dealt with the methodological aspects, but we have often referred to specific applications to which these methods are pertinent. We have examined the similarities of PUM, GFEM and XFEM, along with some of the differences in the early literature. It has become apparent to us in writing this paper that the differences between these methods are fast vanishing. The basic structure of the extrinsic enrichment employed in these methods is identical, and the differences reside largely in the areas of application, the types of enrichment and under which cognomen various developments have been made; however we have used the names employed in the cited papers when describing specific methods or applications.

We have focused on methods for problems with discontinuous gradients, singularities, and other non-smooth features. These methods are of particular importance for this class of problems because they tremendously facilitate their solution: they avoid the need for the finite element mesh to conform to these features, and for evolutionary problems they avoid the need for remeshing. Furthermore, such methods can provide substantially higher accuracy as compared to standard finite element methods for problems with such features.

Although these methods are conceptually elegant and simple, we have shown that many issues require special attention; some of these issues are close to resolution whereas others will still require considerable further research. For example, some localized enrichments lead to difficulties in blending elements; we have classified and described different approaches for resolving these difficulties and reviewed the literature on this topic. A second major issue is the quadrature of the weak form. For discontinuities, we have reviewed methods based on decomposing the elements and those based on regularization, among others. Methods and issues for quadrature of singular functions and higher-order elements, have also been reviewed. Effective quadrature methods that account for singularities curved interfaces are important in many applications. Furthermore, the approximations must be carefully formulated so that inaccuracies do not arise in blending elements.

We have also discussed some of the developments for time stepping schemes in XFEM; these developments are crucial for effective modeling of discontinuities and high gradients across *moving* interfaces. Space-time elements provide a consistent framework for this but are computationally demanding; some other alternatives were reviewed.

The enforcement of boundary and interface conditions has been reviewed, including Lagrange multiplier methods, penalty methods, and Nitsche's method. We also reviewed the issues arising from linear dependence of the basis and ill-conditioning.

Finally, a rather brief but wide overview of the applications of these methods has been interspersed with the various methodologies throughout this paper. We hope that we have conveyed the importance and ubiquitousness of problems with discontinuities, high gradients, and singular or near singular behavior in applications of practical importance. The XFEM and related methods offer a means to address these applications in much simpler ways and also with great accuracy. It is, therefore, our belief that the XFEM and GFEM will eventually be the methods of choice for a wide range of scientific and engineering applications.

ACKNOWLEDGEMENTS

The support of the German Research Foundation (DFG) in the frame of the Emmy-Noether-research group "Numerical methods for discontinuities in continuum mechanics", the support of the Office of Naval Research under Grant N00014-08-1-1191 and the Army Research Office under Grant W911NF-08-1-0212 are gratefully acknowledged.

REFERENCES

1. S. Abbas, A. Alizada, and T.P. Fries. The XFEM for convection-dominated problems. *Internat. J. Numer. Methods Engrg.*, page submitted, 2009.
2. Y. Abdelaziz and A. Hamouine. A survey of the extended finite element. *Computers & Structures*, 86:1141 – 1151, 2008.
3. M. Ainsworth and J.T. Oden. A posteriori error estimation in finite element analysis. *Comp. Methods Appl. Mech. Engrg.*, 142:1 – 88, 1997.
4. M. Ainsworth and J.T. Oden. *A Posteriori Error Estimation in Finite Element Analysis*. John Wiley & Sons, Chichester, 2000.
5. P.M.A. Areias and T. Belytschko. Analysis of three-dimensional crack initiation and propagation using the extended finite element method. *Internat. J. Numer. Methods Engrg.*, 63:760 – 788, 2005.
6. P.M.A. Areias and T. Belytschko. A comment on the article "a finite element method for simulation of strong and weak discontinuities in solid mechanics" by a. hansbo and p. hansbo [comput.methods appl. mech. engrg. 193 (2004) 3523-3540]. *Comp. Methods Appl. Mech. Engrg.*, 195:1275 – 1276, 2006.
7. P.M.A. Areias and T. Belytschko. Two-scale shear band evolution by local partition of unity. *Internat. J. Numer. Methods Engrg.*, 66:878 – 910, 2006.
8. P.M.A. Areias and T. Belytschko. Two-scale method for shear bands: thermal effects and variable bandwidth. *Internat. J. Numer. Methods Engrg.*, 72:658 – 696, 2007.
9. A. Asadpoure and S. Mohammadi. Developing new enrichment functions for crack simulation in orthotropic media by the extended finite element method. *Internat. J. Numer. Methods Engrg.*, 69:2150 – 2172, 2007.
10. J.L. Asferg, P.N. Poulsen, and L.O. Nielsen. A consistent partly cracked XFEM element for cohesive crack growth. *Internat. J. Numer. Methods Engrg.*, 72:464 – 485, 2007.
11. I. Babuška. Error-bounds for finite element method. *Numer. Math.*, 16:322 – 333, 1971.
12. I. Babuška, U. Banerjee, and J.E. Osborn. Survey of meshless and generalized finite element methods: a unified approach. *Acta Numerica*, 12:1 – 125, 2003.
13. I. Babuška, U. Banerjee, and J.E. Osborn. Generalized finite element methods: Main ideas, results and perspectives. *Int. J. Comp. Meth.*, 1:67 – 103, 2004.
14. I. Babuška, G. Caloz, and J.E. Osborn. Special finite element methods for a class of second order elliptic problems with rough coefficients. *SIAM J Numerical Analysis*, 31:945 – 981, 1994.
15. I. Babuška, F. Ihlenburg, E.T. Paik, and S.A. Sauter. A generalized finite element method for solving the Helmholtz equation in two dimensions with minimal pollution. *Comp. Methods Appl. Mech. Engrg.*, 128:325 – 359, 1995.
16. I. Babuška and J.M. Melenk. The partition of unity method. *Internat. J. Numer. Methods Engrg.*, 40:727 – 758, 1997.
17. I. Babuška and J.E. Osborn. Generalized finite element methods: Their performance and their relation to mixed methods. *SIAM J Numerical Analysis*, 20:510 – 536, 1983.
18. G.I. Barenblatt. The mathematical theory of equilibrium of cracks in brittle fracture. *Advan. Appl. Mech.*, 7:55 – 129, 1962.

19. F.B. Barros, S.P.B. Proença, and C.S. de Barcellos. Generalized finite element method in structural nonlinear analysis-a p-adaptive strategy. *Comput. Mech.*, 33:95 – 107, 2004.
20. F.B. Barros, S.P.B. Proença, and C.S. de Barcellos. On error estimator and p-adaptivity in the generalized finite element method. *Internat. J. Numer. Methods Engrg.*, 60:2373 – 2398, 2004.
21. R.S. Barsoum. Application of quadratic isoparametric elements in linear fracture mechanics. *Int. J. of Fracture*, 10:603 – 605, 1974.
22. E. Béchet, H. Minnebo, N. Moës, and B. Burgardt. Improved implementation and robustness study of the X-FEM for stress analysis around cracks. *Internat. J. Numer. Methods Engrg.*, 64:1033–1056, 2005.
23. T. Belytschko and T. Black. Elastic crack growth in finite elements with minimal remeshing. *Internat. J. Numer. Methods Engrg.*, 45:601 – 620, 1999.
24. T. Belytschko, H. Chen, J. Xu, and G. Zi. Dynamic crack propagation based on loss of hyperbolicity and a new discontinuous enrichment. *Internat. J. Numer. Methods Engrg.*, 58:1873 – 1905, 2003.
25. T. Belytschko and R. Gracie. On XFEM applications to dislocations and interfaces. *Int. J. Plast.*, 23:1721 – 1738, 2007.
26. T. Belytschko, R. Gracie, and G. Ventura. A review of extended/generalized finite element methods for material modelling. *Modelling Simul. Mater. Sci. Eng.*, 17:043001, 2009.
27. T. Belytschko, Y. Krongauz, D. Organ, M. Fleming, and P. Krysl. Meshless methods: An overview and recent developments. *Comp. Methods Appl. Mech. Engrg.*, 139:3 – 47, 1996.
28. T. Belytschko, W.K. Liu, and B. Moran. *Nonlinear Finite Elements for Continua and Structures*. John Wiley & Sons, Chichester, 2000.
29. T. Belytschko, N. Moës, S. Usui, and C. Parimi. Arbitrary discontinuities in finite elements. *Internat. J. Numer. Methods Engrg.*, 50:993 – 1013, 2001.
30. T. Belytschko, C. Parimi, N. Moës, N. Sukumar, and S. Usui. Structured extended finite element methods for solids defined by implicit surfaces. *Internat. J. Numer. Methods Engrg.*, 56:609 – 635, 2003.
31. T. Belytschko, S.P. Xiao, and C. Parimi. Topology optimization with implicit functions and regularization. *Internat. J. Numer. Methods Engrg.*, 57:1177 – 1196, 2003.
32. E. Benvenuti. A regularized XFEM framework for embedded cohesive interfaces. *Comp. Methods Appl. Mech. Engrg.*, 197:4367 – 4378, 2008.
33. E. Benvenuti, A. Tralli, and G. Ventura. A regularized XFEM model for the transition from continuous to discontinuous displacements. *Internat. J. Numer. Methods Engrg.*, 74:911 – 944, 2008.
34. S. Bordas and M. Duflot. Derivative recovery and a posteriori error estimate for extended finite elements. *Comp. Methods Appl. Mech. Engrg.*, 196:3381 – 3399, 2007.
35. S. Bordas, M. Duflot, and P. Le. A simple error estimator for extended finite elements. *Commun. Numer. Meth. Engrg.*, 24:961 – 971, 2007.
36. S. Bordas, P.V. Nguyen, C. Dunant, A. Guidoum, and H. Nguyen-Dang. An extended finite element library. *Internat. J. Numer. Methods Engrg.*, 71:703 – 732, 2007.
37. F. Brezzi. On the existence, uniqueness and approximation of saddle-point problems arising from Lagrange multipliers. *RAIRO Anal. Numér.*, R-2:129 – 151, 1974.
38. É. Budyn, G. Zi, N. Moës, and T. Belytschko. A method for multiple crack growth in brittle materials without remeshing. *Internat. J. Numer. Methods Engrg.*, 61:1741 – 1770, 2004.
39. L.P. Franca C. Farhat, I. Harari. The discontinuous enrichment method. *Comp. Methods Appl. Mech. Engrg.*, 190:6455 – 6479, 2001.
40. P. Weidemann-Goiran C. Farhat, R. Tezaur. Higher-order extensions for a discontinuous galerkin methods for mid-frequency helmholtz problems. *Internat. J. Numer. Methods Engrg.*, 61:1938 – 1956, 2004.
41. U. Hetmaniuk C. Farhat, I. Harari. A discontinuous galerkin method with lagrange multipliers for the solution of helmholtz problems in the mid-frequency regime. *Comp. Methods Appl. Mech. Engrg.*, 192:1389 – 1419, 2003.
42. O. Cessenat and B. Despres. Application of an ultra weak variational formulation of elliptic pdes to the two-dimensional helmholtz problem. *SIAM J. Numer. Anal.*, 35:255 – 299, 1998.
43. E. Chahine, P. Laborde, and Y. Renard. Crack tip enrichment in the XFEM using a cutoff function. *Internat. J. Numer. Methods Engrg.*, 75:629 – 646, 2008.
44. G. Chen, Y. Ohnishi, and T. Ito. Development of high-order manifold method. *Internat. J. Numer. Methods Engrg.*, 43:685 – 712, 1998.
45. K.W. Cheng and T.P. Fries. Higher-order XFEM for curved strong and weak discontinuities. *Internat. J. Numer. Methods Engrg.*, page submitted, 2009.
46. J. Chessa and T. Belytschko. An enriched finite element method and level sets for axisymmetric two-phase flow with surface tension. *Internat. J. Numer. Methods Engrg.*, 58:2041 – 2064, 2003.
47. J. Chessa and T. Belytschko. An extended finite element method for two-phase fluids. *ASME J. Appl. Mech.*, 70:10 – 17, 2003.
48. J. Chessa and T. Belytschko. Arbitrary discontinuities in space-time finite elements by level-sets and X-FEM. *Internat. J. Numer. Methods Engrg.*, 61:2595 – 2614, 2004.

49. J. Chessa and T. Belytschko. A local space-time discontinuous finite element method. *Comp. Methods Appl. Mech. Engrg.*, 195:1325 – 1343, 2006.
50. J. Chessa, P. Smolinski, and T. Belytschko. The extended finite element method (XFEM) for solidification problems. *Internat. J. Numer. Methods Engrg.*, 53:1959 – 1977, 2002.
51. J. Chessa, H. Wang, and T. Belytschko. On the construction of blending elements for local partition of unity enriched finite elements. *Internat. J. Numer. Methods Engrg.*, 57:1015 – 1038, 2003.
52. D.L. Chopp and N. Sukumar. Fatigue crack propagation of multiple coplanar cracks with the coupled extended finite element/fast marching method. *Int. J. Engrg. Sci.*, 41:845 – 869, 2003.
53. C. Comi and S. Mariani. Extended finite element simulation of quasi-brittle fracture in functionally graded materials. *Comp. Methods Appl. Mech. Engrg.*, 196:4013 – 4026, 2007.
54. J.V. Cox. An extended finite element method with analytical enrichment for cohesive crack modeling. *Internat. J. Numer. Methods Engrg.*, page DOI: 10.1002/nme.2475, 2009.
55. C. Daux, N. Moës, J. Dolbow, N. Sukumar, and T. Belytschko. Arbitrary branched and intersecting cracks with the extended finite element method. *Internat. J. Numer. Methods Engrg.*, 48:1741 – 1760, 2000.
56. J. Dolbow and I. Harari. An efficient finite element method for embedded interface problems. *Internat. J. Numer. Methods Engrg.*, page DOI: 10.1002/nme.2486, 2009.
57. J. Dolbow, N. Moës, and T. Belytschko. Discontinuous enrichment in finite elements with a partition of unity method. *Finite Elem. Anal. Des.*, 36:235 – 260, 2000.
58. J. Dolbow, N. Moës, and T. Belytschko. Modeling fracture in Mindlin-Reissner plates with the extended finite element method. *J. Solids Struct.*, 37:7161 – 7183, 2000.
59. J. Dolbow, N. Moës, and T. Belytschko. An extended finite element method for modeling crack growth with frictional contact. *Comp. Methods Appl. Mech. Engrg.*, 190:6825 – 6846, 2001.
60. J.E. Dolbow and L.P. Franca. Residual-free bubbles for embedded dirichlet problems. *Comp. Methods Appl. Mech. Engrg.*, 197:3751 – 3759, 2008.
61. J. Donea and A. Huerta. *Finite Element Methods for Flow Problems*. John Wiley & Sons, Chichester, 2003.
62. C.A. Duarte, I. Babuška, and J.T. Oden. Generalized finite element methods for three-dimensional structural mechanics problems. *Computers & Structures*, 77:215 – 232, 2000.
63. C.A. Duarte, O.N. Hamzeh, T.J. Liszka, and W.W. Tworzydlo. A generalized finite element method for the simulation of three-dimensional dynamic crack propagation. *Comp. Methods Appl. Mech. Engrg.*, 190:2227 – 2262, 2001.
64. C.A. Duarte and J.T. Oden. An h-p adaptive method using clouds. *Comp. Methods Appl. Mech. Engrg.*, 139:237 – 262, 1996.
65. C.A. Duarte, L.G. Reno, and A. Simone. A high-order generalized FEM for through-the-thickness branched cracks. *Internat. J. Numer. Methods Engrg.*, 72:325 – 351, 2007.
66. C.A.M. Duarte and J.T. Oden. H-p clouds – an h-p meshless method. *Numer. Methods Partial Differential Equations*, 12:673 – 705, 1996.
67. R. Duddu, S. Bordas, D. Chopp, and B. Moran. A combined extended finite element and level set method for biofilm growth. *Internat. J. Numer. Methods Engrg.*, 74:848 – 870, 2008.
68. M. Duflot. A study of the representation of cracks with level-sets. *Internat. J. Numer. Methods Engrg.*, 70:1261–1302, 2007.
69. M. Duflot and S. Bordas. A posteriori error estimation for extended finite elements by an extended global recovery. *Internat. J. Numer. Methods Engrg.*, 76:1123 – 1138, 2008.
70. D.S. Dugdale. Yielding of steel sheets containing slits. *J. Mech. Phys. Solids*, 8:100 – 104, 1960.
71. T. Elguedj, A. Gravouil, and A. Combescure. Appropriate extended functions for X-FEM simulation of plastic fracture mechanics. *Comp. Methods Appl. Mech. Engrg.*, 195:501 – 515, 2006.
72. C. Farhat, I. Harari, and U. Hetmaniuk. The discontinuous enrichment method for multiscale analysis. *Comp. Methods Appl. Mech. Engrg.*, 192:3195 – 3209, 2003.
73. C.A. Felippa, K.C. Park, and C. Farhat. Partitioned analysis of coupled mechanical systems. *Comp. Methods Appl. Mech. Engrg.*, 190:3247 – 3270, 2001.
74. S. Fernández-Méndez and A. Huerta. Imposing essential boundary conditions in mesh-free methods. *Comp. Methods Appl. Mech. Engrg.*, 193:1257 – 1275, 2004.
75. M. Fleming, Y.A. Chu, B. Moran, and T. Belytschko. Enriched element-free Galerkin methods for crack tip fields. *Internat. J. Numer. Methods Engrg.*, 40:1483 – 1504, 1997.
76. T.P. Fries. A corrected XFEM approximation without problems in blending elements. *Internat. J. Numer. Methods Engrg.*, 75:503 – 532, 2008.
77. T.P. Fries. The intrinsic XFEM for two-fluid flows. *Int. J. Numer. Methods Fluids*, 60:437 – 471, 2009.
78. T.P. Fries and T. Belytschko. The intrinsic XFEM: A method for arbitrary discontinuities without additional unknowns. *Internat. J. Numer. Methods Engrg.*, 68:1358 – 1385, 2006.
79. T.P. Fries and T. Belytschko. The intrinsic partition of unity method. *Comput. Mech.*, 40:803 – 814,

2007.
80. T.P. Fries and H.G. Matthies. Classification and overview of meshfree methods. Informatikbericht-Nr. 2003-03, Technical University Braunschweig, (http://opus.tu-bs.de/opus/volltexte/2003/418/), Brunswick, 2003.
81. T.P. Fries and A. Zilian. On time integration in the XFEM. *Internat. J. Numer. Methods Engrg.*, 79:69 – 93, 2009.
82. L. Gaul, M. Kogl, and M. Wagner. *Boundary Element Methods for Engineers and Scientists*. Springer, Berlin, 2003.
83. A. Gerstenberger and W.A. Wall. Enhancement of fixed-grid methods towards complex fluid-structure interaction applications. *Int. J. Numer. Methods Fluids*, 57:1227 – 1248, 2008.
84. A. Gerstenberger and W.A. Wall. An eXtended finite element method/Lagrange multiplier based approach for fluid-structure interaction. *Comp. Methods Appl. Mech. Engrg.*, 197:1699 – 1714, 2008.
85. E. Giner, N. Sukumar, J.E. Tarancón, and F.J. Fuenmayor. An Abaqus implementation of the extended finite element method. *Eng. Fract. Mech.*, 76:347 – 368, 2009.
86. C.I. Goldstein. The weak element method applied to helmholtz type equations. *Appl. Numer. Math.*, 2:409 – 426, 1986.
87. R. Gracie and T. Belytschko. Concurrently coupled atomistic and XFEM models for dislocations and cracks. *Internat. J. Numer. Methods Engrg.*, 78:354 – 378, 2009.
88. R. Gracie, J. Oswald, and T. Belytschko. On a new extended finite element method for dislocations: Core enrichment and nonlinear formulation. *Journal of the Mechanics and Physics of Solids*, 56:200 – 214, 2008.
89. R. Gracie, G. Ventura, and T. Belytschko. A new fast finite element method for dislocations based on interior discontinuities. *Internat. J. Numer. Methods Engrg.*, 69:423 – 441, 2007.
90. R. Gracie, H. Wang, and T. Belytschko. Blending in the extended finite element method by discontinuous Galerkin and assumed strain methods. *Internat. J. Numer. Methods Engrg.*, 74:1645 – 1669, 2008.
91. A. Gravouil, N. Moës, and T. Belytschko. Non-planar 3D crack growth by the extended finite element and level sets, part II: level set update. *Internat. J. Numer. Methods Engrg.*, 53:2569 – 2586, 2002.
92. M. Griebel and M.A. Schweitzer. A particle-partition of unity method for the solution of elliptic, parabolic and hyperbolic PDEs. *SIAM J. Sci. Comput.*, 22:853 – 890, 2000.
93. M. Griebel and M.A. Schweitzer. A particle-partition of unity method–part ii: Efficient cover construction and reliable integration. *SIAM J. Sci. Comput.*, 23:1655 – 1682, 2002.
94. M. Griebel and M.A. Schweitzer. A particle-partition of unity method–part v: boundary conditions. In S. Hildebrandt and H. Karcher, editors, *Geometric Analysis and Nonlinear Partial Differential Equations*, pages 517 – 540. Springer, Berlin, 2002.
95. S. Groß and A. Reusken. An extended pressure finite element space for two-phase incompressible flows with surface tension. *J. Comput. Phys.*, 224:40 – 58, 2007.
96. A. Hansbo and P. Hansbo. An unfitted finite element method, based on Nitsche's method, for elliptic interface problems. *Comp. Methods Appl. Mech. Engrg.*, 191:5537 – 5552, 2002.
97. A. Hansbo and P. Hansbo. A finite element method for the simulation of strong and weak discontinuities in solid mechanics. *Comp. Methods Appl. Mech. Engrg.*, 193:3523 – 3540, 2004.
98. A. Hillerborg, M. Modéer, and P.E. Petersson. Analysis of crack formation and crack growth in concrete by means of fracture mechanics and finite elements. *Cement and Concrete Research*, 6:773 – 782, 1976.
99. R. Tezaur I. Kalashnikova, C. Farhat. A discontinuous enrichment method for the solution of advection-diffusion problems in high péclet number regimes. *Finite Elem. Anal. Des.*, 45:238 – 250, 2009.
100. E.V. Iarve. Mesh independent modelling of cracks by using higher order shape functions. *Internat. J. Numer. Methods Engrg.*, 56:869 – 882, 2003.
101. L. Jeřábková and T. Kuhlen. Stable cutting of deformable objects in virtual environments using the XFEM. *IEEE Computer Graphics and Applications*, 29:61 – 71, 2009.
102. H. Ji, D. Chopp, and J.E. Dolbow. A hybrid extended finite element/level set method for modeling phase transformations. *Internat. J. Numer. Methods Engrg.*, 54:1209 – 1233, 2002.
103. H. Ji and J.E. Dolbow. On strategies for enforcing interfacial constraints and evaluating jump conditions with the extended finite element method. *Internat. J. Numer. Methods Engrg.*, 61:2508 – 2535, 2004.
104. B.L. Karihaloo and Q.Z. Xiao. Modelling of stationary and growing cracks in FE framework without remeshing: a state-of-the-art review. *Computers & Structures*, 81:119 – 129, 2003.
105. T.Y. Kim, J. Dolbow, and T. Laursen. A mortared finite element method for frictional contact on arbitrary interfaces. *Comput. Mech.*, 39:223 – 235, 2007.
106. Y. Krongauz and T. Belytschko. EFG approximations with discontiuous derivatives. *Internat. J. Numer. Methods Engrg.*, 41:1215 – 1233, 1998.
107. C. Farhat L. Zhang, R. Tezaur. The discontinuous enrichment method for elastic wave propagation in the medium-frequency regime. *Internat. J. Numer. Methods Engrg.*, 66:2086 – 2114, 2006.
108. P. Laborde, J. Pommier, Y. Renard, and M. Salaün. High-order extended finite element method for

cracked domains. *Internat. J. Numer. Methods Engrg.*, 64:354 – 381, 2005.
109. P. Ladevèze. *Nonlinear Computational Structural Mechanics*. Springer, Berlin, 1998.
110. P. Lancaster and K. Salkauskas. Surfaces generated by moving least squares methods. *Math. Comput.*, 37:141 – 158, 1981.
111. A. Legay, J. Chessa, and T. Belytschko. An Eulerian-Lagrangian method for fluid-structure interaction based on level sets. *Comp. Methods Appl. Mech. Engrg.*, 195:2070 – 2087, 2006.
112. A. Legay and A. Tralli. An euler-lagrange enriched finite element approach for fluid-structure interaction. *European Journal of Computational Mechanics*, 16:145 – 160, 2007.
113. A. Legay, H.W. Wang, and T. Belytschko. Strong and weak arbitrary discontinuities in spectral finite elements. *Internat. J. Numer. Methods Engrg.*, 64:991 – 1008, 2005.
114. F. Liu and R.I. Borja. A contact algorithm for frictional crack propagation with the extended finite element method. *Internat. J. Numer. Methods Engrg.*, 76:1489 – 1512, 2008.
115. X.Y. Liu, Q.Z. Xiao, and B.L. Karihaloo. XFEM for direct evaluation of mixed mode SIFs in homogeneous and bi-materials. *Internat. J. Numer. Methods Engrg.*, 59:1103 – 1118, 2004.
116. S. Mariani and U. Perego. Extended finite element method for quasi-brittle fracture. *Internat. J. Numer. Methods Engrg.*, 58:103 – 126, 2003.
117. J.M. Melenk and I. Babuška. The partition of unity finite element method: basic theory and applications. *Comp. Methods Appl. Mech. Engrg.*, 139:289 – 314, 1996.
118. T. Menouillard, J. Réthoré, A. Combescure, and H. Bung. Efficient explicit time stepping for the eXtended finite element method (X-FEM). *Internat. J. Numer. Methods Engrg.*, 68:911 – 939, 2006.
119. T. Menouillard, J. Réthoré, N. Moës, A. Combescure, and H. Bung. Mass lumping strategies for X-FEM explicit dynamics: Application to crack propagation. *Internat. J. Numer. Methods Engrg.*, 74:447 – 474, 2008.
120. J. Mergheim, E. Kuhl, and P. Steinmann. A hybrid discontinuous Galerkin/interface method for the computational modeling of failure. *Commun. Numer. Meth. Engrg.*, 20:511 – 519, 2004.
121. R. Merle and J. Dolbow. Solving thermal and phase change problems with the eXtended finite element method. *Comput. Mech.*, 28:339 – 350, 2002.
122. G. Meschke and P. Dumstorff. Energy-based modeling of cohesive and cohesionless cracks via X-FEM. *Comp. Methods Appl. Mech. Engrg.*, 196:2338 – 2357, 2007.
123. N. Moës, E. Béchet, and M. Tourbier. Imposing Dirichlet boundary conditions in the extended finite element method. *Internat. J. Numer. Methods Engrg.*, 67:1641 – 1669, 2006.
124. N. Moës and T. Belytschko. Extended finite element method for cohesive crack growth. *Eng. Fract. Mech.*, 69:813 – 833, 2002.
125. N. Moës, M. Cloirec, P. Cartraud, and J.F. Remacle. A computational approach to handle complex microstructure geometries. *Comp. Methods Appl. Mech. Engrg.*, 192:3163–3177, 2003.
126. N. Moës, J. Dolbow, and T. Belytschko. A finite element method for crack growth without remeshing. *Internat. J. Numer. Methods Engrg.*, 46:131 – 150, 1999.
127. N. Moës, A. Gravouil, and T. Belytschko. Non-planar 3D crack growth by the extended finite element and level sets, part I: mechanical model. *Internat. J. Numer. Methods Engrg.*, 53:2549 – 2568, 2002.
128. S. Mohammadi. *Extended finite element method for fracture analysis of structures*. Blackwell, Oxford, 2008.
129. P. Monk and Da-Qing Wang. A least-squares method for the helmholtz equation. *Comp. Methods Appl. Mech. Engrg.*, 175:121 – 136, 1999.
130. C.D. Mote. Global-local finite element. *Internat. J. Numer. Methods Engrg.*, 3:565 – 574, 1971.
131. H.M. Mourad, J. Dolbow, and I. Harari. A bubble-stabilized finite element method for dirichlet constraints on embedded interfaces. *Internat. J. Numer. Methods Engrg.*, 69:772 – 793, 2007.
132. S. Natarajan, S. Bordas, and D.R. Mahapatra. Polygonal finite element method using schwarz christoffel mapping. *Internat. J. Numer. Methods Engrg.*, page accepted, 2009.
133. I. Nistor, O. Pantalé, and S. Caperaa. Numerical implementation of the eXtended finite element method for dynamic crack analysis. *Adv. Eng. Softw*, 39:573 – 587, 2008.
134. A.K. Noor. Global-local methodologies and their applications to nonlinear analysis. *Finite Elem. Anal. Des.*, 2:333 – 346, 1986.
135. J.T. Oden and H.J. Brauchli. On the calculation of consistent stress distributions in finite element approximations. *Internat. J. Numer. Methods Engrg.*, 3:317 – 325, 1971.
136. J.T. Oden, C.A.M. Duarte, and O.C. Zienkiewicz. A new cloud-based hp finite element method. *Comp. Methods Appl. Mech. Engrg.*, 153:117 – 126, 1998.
137. S. Osher and R.P. Fedkiw. Level set methods: an overview and some recent results. *J. Comput. Phys.*, 169:463 – 502, 2001.
138. S. Osher and R.P. Fedkiw. *Level Set Methods and Dynamic Implicit Surfaces*. Springer, Berlin, 2003.
139. J. Oswald, R. Gracie, R. Khare, and T. Belytschko. An extended finite element method for dislocations in complex geometries: Thin films and nanotubes. *Comp. Methods Appl. Mech. Engrg.*, page DOI:

10.1016/j.cma.2008.12.025, 2009.
140. R. Tezaur P. Massimi and C. Farhat. A discontinuous enrichment method for three-dimensional multiscale harmonic wave propagation problems in multi-fluid and fluid-solid media. *Internat. J. Numer. Methods Engrg.*, 76:400 – 425, 2008.
141. K. Park, J.P. Pereira, C.A. Duarte, and G.H. Paulino. Integration of singular enrichment functions in the generalized/extended finite element method for three-dimensional problems. *Internat. J. Numer. Methods Engrg.*, page DOI: 10.1002/nme.2530, 2009.
142. B. Patzák and M. Jirásek. Process zone resolution by extended finite elements. *Eng. Fract. Mech.*, 70:957 – 977, 2003.
143. D. Peng, B. Merriman, S. Osher, H. Zhao, and M. Kang. A PDE-based fast local level set method. *J. Comput. Phys.*, 155:410–438, 1999.
144. J.P. Pereira, C.A. Duarte, D. Guoy, and X. Jiao. hp-Generalized FEM and crack surface representation for non-planar 3-D cracks. *Internat. J. Numer. Methods Engrg.*, 77:601 – 633, 2009.
145. C. Farhat R. Tezaur. Three-dimensional discontinuous galerkin elements with plane waves and lagrange multipliers for the solution of mid-frequency helmholtz problems. *Internat. J. Numer. Methods Engrg.*, 66:796 – 815, 2005.
146. T. Rabczuk, S. Bordas, and G. Zi. On three-dimensional modelling of crack growth using partition of unity methods. *Computers & Structures*, page DOI: 10.1016/j.compstruc.2008.08.010, 2009.
147. B.N. Rao and S. Rahman. An enriched meshless method for non-linear fracture mechanics. *Internat. J. Numer. Methods Engrg.*, 59:197 – 223, 2004.
148. J.J.C. Remmers, R. de Borst, and A. Needleman. A cohesive segments method for the simulation of crack growth. *Comput. Mech.*, 31:69 – 77, 2003.
149. J. Réthoré, A. Gravouil, and A. Combescure. A combined space-time extended finite element method. *Internat. J. Numer. Methods Engrg.*, 64:260 – 284, 2005.
150. J. Réthoré, A. Gravouil, and A. Combescure. An energy-conserving scheme for dynamic crack growth using the eXtended finite element method. *Internat. J. Numer. Methods Engrg.*, 63:631 – 659, 2005.
151. J. Réthoré, F. Hild, and S. Roux. Shear-band capturing using a multiscale extended digital image correlation technique. *Comp. Methods Appl. Mech. Engrg.*, 196:5016 – 5030, 2007.
152. J.J. Ródenas, O.A. González-Estrada, J.E. Tarancón, and F.J. Fuenmayor. A recovery-type error estimator for the extended finite element method based on singular+smooth stress field splitting. *Internat. J. Numer. Methods Engrg.*, 76:545 – 571, 2008.
153. M.E. Rose. Weak element approximations to elliptic differential equations. *Numer. Math.*, 24:185 – 204, 1975.
154. G. Russo and P. Smereka. A remark on computing distance functions. *J. Comput. Phys.*, 163:51 – 67, 2000.
155. E. Samaniego and T. Belytschko. Continuum-discontinuum modelling of shear bands. *Internat. J. Numer. Methods Engrg.*, 62:1857 – 1872, 2005.
156. M.A. Schweitzer. *Mesh-free and generalized finite element methods*. Habilitation, Institute for Numerical Simulation, University of Bonn, Germany, 2008.
157. J.A. Sethian. A fast marching level set method for monotonically advancing fronts. *Proc. Nat. Acad. Sci.*, 93:1591 – 1595, 1996.
158. J.A. Sethian. Fast marching methods. *SIAM Review*, 41:199 – 235, 1999.
159. J.A. Sethian. *Level Set Methods and Fast Marching Methods*. Cambridge University Press, Cambridge, 2 edition, 1999.
160. D. Shepard. A two-dimensional interpolation function for irregularily spaced points. In *Proceedings of the 23rd Nat. Conf. ACM*, pages 517 – 523, USA, 1968.
161. G. Shi. Manifold method of material analysis. In *Trans. 9th Army Conf. on Applied Mathematics and Computing*, pages 51 – 76, Minneapolis, Minnesota, 1992.
162. A. Simone, C.A. Duarte, and E. Van der Giessen. A generalized finite element method for polycrystals with discontinuous grain boundaries. *Internat. J. Numer. Methods Engrg.*, 67:1122 – 1145, 2006.
163. B.G. Smith, B.L. Vaughan Jr., and D.L. Chopp. The extended finite element method for boundary layer problems in biofilm growth. *Comm. App. Math. and Comp. Sci.*, 2:35 – 56, 2007.
164. J.H. Song and T. Belytschko. Cracking node method for dynamic fracture with finite elements. *Internat. J. Numer. Methods Engrg.*, 77:360 – 385, 2009.
165. F.L. Stazi, E. Budyn, J. Chessa, and T. Belytschko. An extended finite element method with higher-order elements for curved cracks. *Comput. Mech.*, 31:38 – 48, 2003.
166. M. Stolarska and D.L. Chopp. Modeling thermal fatigue cracking in integrated circuits by level sets and the extended finite element method. *Int. J. Engrg. Sci.*, 41:2381 – 2410, 2003.
167. M. Stolarska, D.L. Chopp, N. Moës, and T. Belytschko. Modelling crack growth by level sets in the extended finite element method. *Internat. J. Numer. Methods Engrg.*, 51:943 – 960, 2001.
168. J. Strain. Fast tree-based redistancing for level set computations. *J. Comput. Phys.*, 152:664 – 686,

1999.
169. T. Strouboulis, I. Babuška, and K. Copps. The design and analysis of the generalized finite element method. *Comp. Methods Appl. Mech. Engrg.*, 181:43 – 69, 2000.
170. T. Strouboulis, I. Babuška, and R. Hidajat. The generalized finite element method for Helmholtz equation: theory, computation, and open problems. *Comp. Methods Appl. Mech. Engrg.*, 195:4711 – 4731, 2006.
171. T. Strouboulis, K. Copps, and I. Babuška. The generalized finite element method: an example of its implementation and illustration of its performance. *Internat. J. Numer. Methods Engrg.*, 47:1401 – 1417, 2000.
172. T. Strouboulis, K. Copps, and I. Babuška. The generalized finite element method. *Comp. Methods Appl. Mech. Engrg.*, 190:4081 – 4193, 2001.
173. T. Strouboulis, R. Hidajat, and I. Babuška. The generalized finite element method for Helmholtz equation, part II: effect of choice of handbook functions, error due to absorbing boundary conditions and its assessment. *Comp. Methods Appl. Mech. Engrg.*, 197:364 – 380, 2008.
174. T. Strouboulis, L. Zhang, and I. Babuška. Generalized finite element method using mesh-based handbooks: application to problems in domains with many voids. *Comp. Methods Appl. Mech. Engrg.*, 192:3109 – 3161, 2003.
175. T. Strouboulis, L. Zhang, and I. Babuška. p-version of the generalized FEM using mesh-based handbooks with applications to multiscale problems. *Internat. J. Numer. Methods Engrg.*, 60:1639 – 1672, 2004.
176. T. Strouboulis, L. Zhang, D. Wang, and I. Babuška. A posteriori error estimation for generalized finite element methods. *Comp. Methods Appl. Mech. Engrg.*, 195:852 – 879, 2006.
177. N. Sukumar, D.L. Chopp, E. Béchet, and N. Moës. Three-dimensional non-planar crack growth by a coupled extended finite element and fast marching method. *Internat. J. Numer. Methods Engrg.*, 76:727 – 748, 2008.
178. N. Sukumar, D.L. Chopp, N. Moës, and T. Belytschko. Modeling holes and inclusions by level sets in the extended finite-element method. *Comp. Methods Appl. Mech. Engrg.*, 190:6183 – 6200, 2001.
179. N. Sukumar, D.L. Chopp, and B. Moran. Extended finite element method and fast marching method for three-dimensional fatigue crack propagation. *Eng. Fract. Mech.*, 70:29 – 48, 2003.
180. N. Sukumar, N. Moës, B. Moran, and T. Belytschko. Extended finite element method for three-dimensional crack modelling. *Internat. J. Numer. Methods Engrg.*, 48:1549 – 1570, 2000.
181. N. Sukumar and J.H. Prévost. Modeling quasi-static crack growth with the extended finite element method, part I: computer implementation. *J. Solids Struct.*, 40:7513 – 7537, 2003.
182. M. Sussman and E. Fatemi. An efficient interface-preserving level set redistancing algorithm and its application to interfacial incompressible fluid flow. *SIAM J. Sci. Comput.*, 20:1165 – 1191, 1999.
183. A. Sutradhar, G.H. Paulino, and L.J. Gray. *Symmetric Galerkin Boundary Element Method*. Springer, Berlin, 2008.
184. M. Tabbara, T. Blacker, and T. Belytschko. Finite element derivative recovery by moving least square interpolants. *Comp. Methods Appl. Mech. Engrg.*, 117:211 – 223, 1994.
185. J.E. Tarancón, A. Vercher, E. Giner, and F. J. Fuenmayor. Enhanced blending elements for XFEM applied to linear elastic fracture mechanics. *Internat. J. Numer. Methods Engrg.*, 77:126 – 148, 2009.
186. J.F. Unger, S. Eckardt, and C. Könke. Modelling of cohesive crack growth in concrete structures with the extended finite element method. *Comp. Methods Appl. Mech. Engrg.*, 196:4087 – 4100, 2007.
187. S.P. van der Pijl, A. Segal, C. Vuik, and P. Wesseling. A mass-conserving level-set method for modelling of multi-phase flows. *Int. J. Numer. Methods Fluids*, 47:339 – 361, 2005.
188. G. Ventura. On the elimination of quadrature subcells for discontinuous functions in the eXtended finite element method. *Internat. J. Numer. Methods Engrg.*, 66:761 – 795, 2006.
189. G. Ventura, E. Budyn, and T. Belytschko. Vector level sets for description of propagating cracks in finite elements. *Internat. J. Numer. Methods Engrg.*, 58:1571 – 1592, 2003.
190. G. Ventura, R. Gracie, and T. Belytschko. Fast integration and weight function blending in the extended finite element method. *Internat. J. Numer. Methods Engrg.*, 77:1 – 29, 2009.
191. G. Ventura, B. Moran, and T. Belytschko. Dislocations by partition of unity. *Internat. J. Numer. Methods Engrg.*, 62:1463 – 1487, 2005.
192. G. Ventura, J.X. Xu, and T. Belytschko. A vector level set method and new discontinuity approximations for crack growth by EFG. *Internat. J. Numer. Methods Engrg.*, 54:923 – 944, 2002.
193. L.M. Vigneron, J.G. Verly, and S.K. Warfield. On extended finite element method (XFEM) for modelling of organ deformations associated with surgical cuts. In S. Cotin and D. Metaxas, editors, *Medical Simulation*, volume 3078 of *Lecture Notes in Computer Science*. Springer, Berlin, 2004.
194. G.J. Wagner, N. Moës, W.K. Liu, and T. Belytschko. The extended finite element method for rigid particles in Stokes flow. *Internat. J. Numer. Methods Engrg.*, 51:293 – 313, 2001.
195. H. Waisman and T. Belytschko. Parametric enrichment adaptivity by the extended finite element method. *Internat. J. Numer. Methods Engrg.*, 73:1671 – 1692, 2008.

196. G.N. Wells and L.J. Sluys. A new method for modelling cohesive cracks using finite elements. *Internat. J. Numer. Methods Engrg.*, 50:2667 – 2682, 2001.
197. G.N. Wells, L.J. Sluys, and R. de Borst. Simulating the propagation of displacement discontinuities in a regularized strain-softening medium. *Internat. J. Numer. Methods Engrg.*, 53:1235 – 1256, 2002.
198. M.L. Williams. The bending stress distribution at the base of a stationary crack. *J. Appl. Mech., ASME*, 28:78 – 82, 1961.
199. Q.Z. Xiao and B.L. Karihaloo. Direct evaluation of accurate coefficients of the linear elastic crack tip asymptotic field. *Fatigue & Fracture of Engineering Materials & Structures*, 26:719 – 729, 2003.
200. Q.Z. Xiao and B.L. Karihaloo. Improving the accuracy of XFEM crack tip fields using higher order quadrature and statically admissible stress recovery. *Internat. J. Numer. Methods Engrg.*, 66:1378 – 1410, 2006.
201. Q.Z. Xiao, B.L. Karihaloo, and X.Y. Liu. Incremental-secant modulus iteration scheme and stress recovery for simulating cracking process in quasi-brittle materials using XFEM. *Internat. J. Numer. Methods Engrg.*, 69:2606 – 2635, 2007.
202. G. Zi and T. Belytschko. New crack-tip elements for XFEM and applications to cohesive cracks. *Internat. J. Numer. Methods Engrg.*, 57:2221 – 2240, 2003.
203. O.C. Zienkiewicz and R.L. Taylor. *The Finite Element Method*, volume 1 – 3. Butterworth-Heinemann, Oxford, 2000.
204. O.C. Zienkiewicz and J.Z. Zhu. The superconvergent patch recovery and a posteriori error estimates. Part I: the recovery technique. *Internat. J. Numer. Methods Engrg.*, 33:1331 – 1364, 1992.
205. O.C. Zienkiewicz and J.Z. Zhu. The superconvergent patch recovery and a posteriori error estimates. Part II: error estimates and adaptivity. *Internat. J. Numer. Methods Engrg.*, 33:1365 – 1382, 1992.
206. A. Zilian and T.P. Fries. A localized mixed-hybrid method for imposing interfacial constraints in the extended finite element method (XFEM). *Internat. J. Numer. Methods Engrg.*, page DOI: 10.1002/nme.2596, 2009.
207. A. Zilian and A. Legay. The enriched space-time finite element method (EST) for simultaneous solution of fluid-structure interaction. *Internat. J. Numer. Methods Engrg.*, 75:305–334, 2008.